



**CENTRO DE INVESTIGACIÓN Y DE ESTUDIOS  
AVANZADOS DEL INSTITUTO POLITÉCNICO  
NACIONAL**

Unidad Zacatenco  
Departamento de Control Automático

**"Estabilidad de la ecuación de Hill.  
Un enfoque de Sturm-Liouville"**

T E S I S

Que presenta

Ing. Néstor Abraham Aguillón Balderas

Para obtener el grado de

**MAESTRO EN CIENCIAS**

En la especialidad de

**CONTROL AUTOMÁTICO**

Director de la Tesis:  
Dr. Joaquín Collado Moctezuma



I would like to dedicate this thesis to my loving parents ...



## **Acknowledgements**

I would like to acknowledge:

Dr. Collado, for its patience, advises and guidance.

My parents, for all their love and support.

My girlfriend, for all her love and encouragement.

CONACYT for my studentship.



# Abstract

Using periodic and anti-periodic boundary conditions, the Ince-Strutt diagram of the  $T$ -periodic Hill equation is computed. A generalization of these two boundary conditions, known as *twisted boundary conditions*, is used in order to find the parameter regions where  $kT$ -periodic and aperiodic solutions exist. The boundary value problem associated to each of these boundary conditions is set as a Sturm-Liouville problem, which is the eigenvalue problem of a linear differential self-adjoint operator, whose spectra, as it is shown by the Sturm-Liouville theory, consists of a monotonic sequence of real numbers. An arbitrary order finite-difference scheme is proposed for the approximate solution of these Sturm-Liouville problems. The obtained results are compared with others obtained by two other methods. An academic example is given to show how this approach can be applied to other second order bi-parametric periodic equations which are not on a Hill type form.





# Resumen

Usando condiciones de frontera periódicas y anti-periódicas, se calcula, de forma aproximada, el diagrama de Ince-Strutt de la ecuación de Hill de periodo  $T$ . Una generalización de estos dos tipos de condiciones de contorno, conocida como condiciones de frontera torcidas, es utilizada para encontrar las regiones de parámetros en las que dicha ecuación presenta soluciones periódicas de periodo  $kT$ , donde  $k$  es un número entero positivo. La solución de cada uno de estos problemas se define como un problema de Sturm-Liouville, que a su vez corresponde a un problema de valores y vectores propios de un operador diferencial lineal. El espectro de este operador, como lo prueba la teoría de Sturm-Liouville, forma una secuencia monótona de números reales. Se propone un esquema basado en diferencias finitas para la solución aproximada de estos problemas. Los resultados obtenidos son comparados con aquellos recabados por otros dos métodos. Un ejemplo académico es dado para mostrar cómo este enfoque puede ser aplicado a ecuaciones periódicas bi-paramétricas de segundo orden que no se encuentran en una forma de tipo Hill.



# Table of contents

<b>Abstract</b>	<b>vii</b>
<b>Resumen</b>	<b>ix</b>
<b>List of figures</b>	<b>xiii</b>
<b>List of tables</b>	<b>xv</b>
<b>List of abbreviations and symbols</b>	<b>xvii</b>
<b>1 Introduction</b>	<b>1</b>
<b>2 Background</b>	<b>7</b>
2.1 Floquet theory . . . . .	7
2.2 Linear Hamiltonian systems . . . . .	10
2.3 Reducibility . . . . .	12
<b>3 Hill equation</b>	<b>15</b>
3.1 Preliminaries . . . . .	15
3.2 Periodic and aperiodic solutions . . . . .	18
3.3 Stability . . . . .	22
3.3.1 Damping . . . . .	23
3.4 Reducibility . . . . .	24
3.5 Coexistence . . . . .	26
3.5.1 Lamé equation . . . . .	26
<b>4 Sturm-Liouville theory</b>	<b>27</b>
4.1 Sturm-Liouville equation . . . . .	27
4.2 Sturm-Liouville BCs . . . . .	28
4.2.1 Twisted, periodic and anti-periodic BCs . . . . .	29

4.3	Sturm-Liouville problem . . . . .	30
4.3.1	Linear space of the Sturm-Liouville problem . . . . .	30
4.3.2	Sturm-Liouville operator . . . . .	30
4.3.3	Periodic and antiperiodic Sturm-Liouville problem . . . . .	32
4.3.4	Twisted Sturm-Liouville problem . . . . .	34
<b>5</b>	<b>The Sturm-Liouville problem and the Hill equation</b>	<b>37</b>
5.1	Finite difference scheme for the twisted Sturm-Liouville problem . . . . .	37
5.2	Stability chart . . . . .	41
5.3	Splitting lines . . . . .	44
5.3.1	Splitting lines of periodic solutions . . . . .	44
5.3.2	Splitting lines of aperiodic bounded solutions . . . . .	46
5.3.3	Linear resonance . . . . .	46
5.4	Addition of damping . . . . .	48
5.5	Lamé equation . . . . .	50
5.6	Quasi-periodic Hill equation . . . . .	52
5.7	Comparative study . . . . .	53
<b>6</b>	<b>A mechanical system with periodically varying moment of inertia</b>	<b>57</b>
6.1	Linear model . . . . .	57
6.2	Bifurcation diagram . . . . .	58
<b>7</b>	<b>An application of the Mathieu equation</b>	<b>61</b>
7.1	Quadrupole mass filter . . . . .	61
7.1.1	Ion equations of motion . . . . .	61
7.1.2	Filtering principle . . . . .	64
<b>8</b>	<b>Conclusions and future work</b>	<b>67</b>
8.1	Conclusions . . . . .	67
8.2	Future work . . . . .	68
	<b>Bibliography</b>	<b>69</b>

# List of figures

1.1	Ince-Strutt diagram . . . . .	3
5.1	Stability chart of the Mathieu equation . . . . .	42
5.2	Stability chart of the Meissner equation . . . . .	43
5.3	Stability chart of the Hill equation with $f(t) = \frac{d}{q} \left( \frac{1}{(1.1+\cos(t))} - m \right)$ . . . . .	43
5.4	Stability chart of the Mathieu equation with splitting lines correspondent to $10\pi$ -periodic solutions. . . . .	45
5.5	$10\pi$ -periodic solution of the Mathieu equation for initial condition $x(0) = [1, 0]^T$ and computed parameters $\alpha = 2.821159061221791$ and $\beta = 2$ for Floquet multipliers $\mu_{1,2} = e^{\pm j2\pi(2/5)}$ . . . . .	45
5.6	Stability chart of the Mathieu equation with splitting lines correspondent to aperiodic solutions. . . . .	46
5.7	Aperiodic solution of the Mathieu equation for initial condition $x(t) = [1, 0]^T$ and computed parameters $\alpha = 1.781357855842370$ and $\beta = 2$ for Floquet multipliers $\mu_{1,2} = e^{\pm j2\pi^2}$ . . . . .	47
5.8	Resonant aperiodic solution of Mathieu's equation with forcing input $u(t) = \cos(\sqrt{2}t)$ , initial condition $x(t) = [0.05, 0]^T$ , and computed parameters $\alpha = 2.787354403706198$ and $\beta = 2$ for Floquet multipliers $\mu_{1,2} = e^{\pm j2\pi\sqrt{2}}$ . . . . .	48
5.9	Resonant aperiodic solution of Mathieu's equation with forcing input $u(t) = \cos((\sqrt{2} + 1)t)$ , initial condition $x(t) = [0.05, 0]^T$ , and computed parameters $\alpha = 2.787354403706198$ and $\beta = 2$ for Floquet multipliers $\mu_{1,2} = e^{\pm j2\pi\sqrt{2}}$ . . . . .	49
5.10	Stability charts of damped Mathieu's equation for three different damping coefficient values . . . . .	50
5.11	Ince-Strutt diagram of the Lamé equation . . . . .	51
5.12	Diagram obtained by solving the periodic and the anti-periodic Sturm-Liouville problems for the quasi-periodic Hill equation (5.14), for $f(t) = \cos(t) + 0.2 \sin(2\pi t)$ . . . . .	52
5.13	Superimposition of the diagrams in Figures 5.12 and 5.1. . . . .	53

---

5.14	Ince-Strutt diagram of the Mathieu equation correspondent to Table 5.1 . . .	54
5.15	Ince-Strutt diagram of the Mathieu equation correspondent to Table 5.3 . . .	54
6.1	Elastic shaft with a rigid disk with two radially moving masses. (image borrowed from [22]) . . . . .	58
6.2	Bifurcation diagram for the elastic shaft system. . . . .	59
6.3	Unbounded solution for the elastic shaft system. . . . .	60
6.4	Bounded solution for the elastic shaft system. . . . .	60
7.1	Schematic of the quadrupole ion mass spectrometer (image borrowed and modified from [23]). . . . .	62
7.2	Ideal shaped electrodes for the potential (7.1) (image borrowed from [23]). .	63
7.3	Equipotential lines for a quadrupole field with the potential (7.1) (image borrowed from [23]). . . . .	63
7.4	Ince-Strutt diagram of the quadrupole mass filter . . . . .	65
7.5	Filter calibration line . . . . .	66

# List of tables

5.1	Some values of the Ince-Strutt diagram obtained using the spectral method algorithm . . . . .	55
5.2	Some values of the Ince-Strutt diagram of the Mathieu equation obtained by Jazar . . . . .	55
5.3	Some values of the Ince-Strutt diagram of the Mathieu equation obtained using the finite-difference scheme with $N = 300$ and $n = 2$ . . . . .	56
5.4	Some values of the Ince-Strutt diagram obtained using the finite-difference scheme with $N = 300$ and $n = 5$ . . . . .	56





# List of abbreviations and symbols

BC	Boundary condition.
BVP	Boundary value problem.
$\sigma(M)$	Spectrum of $M$ .
$\text{tr}(M)$	The trace of matrix $M$ .
$\exp(a)$	Exponential of $a$ . Interchangeable with $e^a$ .
$\ln(a)$	Natural logarithm of $a$ .
$\text{Im}(a)$	Imaginary part of $a$ .
$\text{Re}(a)$	Real part of $a$ .
$\mathring{D}$	Open disc of unitary radius $\triangleq \{s \in \mathbb{C} :  s  < 1\}$
$\bar{D}$	Closed disc of unitary radius $\triangleq \{s \in \mathbb{C} :  s  \leq 1\}$
$L^2$	Space of square integrable functions.
$L^2_{SL}$	Space of square integrable functions that satisfy the Sturm-Liouville BCs.
$ f\rangle$	Element $f$ of a function space, in Dirac's notation.
$\langle f g\rangle$	Inner product of $f$ and $g$ , in Dirac's notation.
$ f $	Norm of $f$ .



# Chapter 1

## Introduction

The term *Hill equation* defines the class of homogeneous, linear, second order ordinary differential equations with real, periodic coefficients [1] which can be reduced to an equation of the form:

$$\ddot{y} + h(t)y = 0, \quad h(t) = h(t + T). \quad (1.1)$$

which can be rewritten as

$$\ddot{y} + \left( a_0 + \sum_{n=1}^{\infty} \left[ a_n \cos\left(\frac{2n\pi}{T}\right) + b_n \sin\left(\frac{2n\pi}{T}\right) \right] \right) y = 0, \quad (1.2)$$

where  $\{a_n\}$  and  $\{b_n\}$  are the Fourier coefficients of  $h(t)$ . This equation received its name in view of the important contribution made by G. W. Hill [2] to their theory while studying the motions of the moon, although such differential equations had been investigated before by Floquet [3], among others.

The Hill equation appears in many applications in science and engineering, where, in the later, the phenomenon known as parametric resonance is of special interest.

Parametric resonance is the instability caused by parametric excitation, i.e. by the periodic variation of a parameter in a dynamical system. For its study, it is common practice to work with the bi-parametric Hill equation

$$\ddot{y} + (\alpha + \beta f(t))y = 0, \quad (1.3)$$

where  $f(t)$  is a zero-mean function that is called the excitation function, and parameters  $\alpha$  and  $\beta$  are functions of the frequency and amplitude of the excitation. For example, in reference [4] is given a model of a pendulum of length  $l$ , subject to parametric excitation introduced

by  $l(t) = l_0 + \varepsilon \cos(\omega t)$ , which, after a time rescaling  $\tau = \omega t$ , gives rise to an equation of the form (1.3) with  $f(t) = \cos(t)$ ,  $\alpha = \omega_0^2/\omega^2$  and  $\beta = \varepsilon\omega_0^2/\omega^2$ , where  $\omega_0 = \sqrt{g/l_0}$  is the natural frequency of the linearized pendulum model in the absence of parametric excitation,  $g$  is the acceleration of gravity, and  $\omega$  and  $\varepsilon$  are, respectively, the frequency and amplitude of the parametric excitation.

Parametric excitation differs from direct forcing in that the excitation appears as the temporal modulation of a parameter rather than as a direct additive input as in:

$$\ddot{y} + \alpha y = \beta f(t). \quad (1.4)$$

Champneys [4] points out that an interesting contrast between these two cases arises in the nature of the trivial response to a non-zero input. For any  $\alpha$  and  $\beta$ , (1.3) admits the trivial solution  $y(t) \equiv 0$ , whereas there is no such solution to (1.4) for non-zero  $\beta$ . So any analysis of a parametrically excited system should start with an analysis of the steady state  $y = 0$ .

It is usual to highlight graphically, through a bifurcation diagram known as the *Ince-Strutt diagram*, the values of  $\alpha$  and  $\beta$  for which the trivial solution of (1.3) is stable or unstable, or equivalently, where solutions stay bounded or become unbounded. Figure 1.1 shows the Ince-Strutt diagram of (1.3) where  $f(t) = \beta \cos(t)$ , which is known as the Mathieu equation. Here, painted areas are known as *Arnold tongues*, and are associated with unbounded solutions, whilst white ones with bounded solutions. The boundaries of the Arnold tongues are known as the *transition curves* of the system, and are associated, in general, with unbounded solutions, excepting at points inside these curves where the width of an Arnold tongue becomes zero for a certain value of  $\beta$ , as, for example, point (5,4) in Figure 1.1. This later case is known as the phenomenon of coexistence, and the point where this happens is called a coexistence point.

Since the solution of a time-varying equation is, in most cases, difficult to obtain, the Arnold tongues of a dynamical system (1.3) are usually obtained through the numeric computation of its transition curves. For this task, it is usually chosen a desired homogeneous grid of values for  $\beta$ , and then, for each value on the grid, the correspondent values of  $\alpha$  inside the transition curves are computed. Floquet theory shows that these values of  $\alpha$  correspond, in fact, to those values for which a periodic solution of period  $T$  or  $2T$  exist.

Among the classical analytic methods for the computation of the Ince-Strutt diagram of a system is the method of infinite determinants, introduced by Hill, and the perturbation method [5], where the approximations of the later are obtained assuming  $\beta$  small. On the other hand, a classical numerical method consists the numerical computation of the state transition matrix of the system to predict boundedness of solutions for fixed values of  $\alpha$  and  $\beta$ , a highly time consuming method.

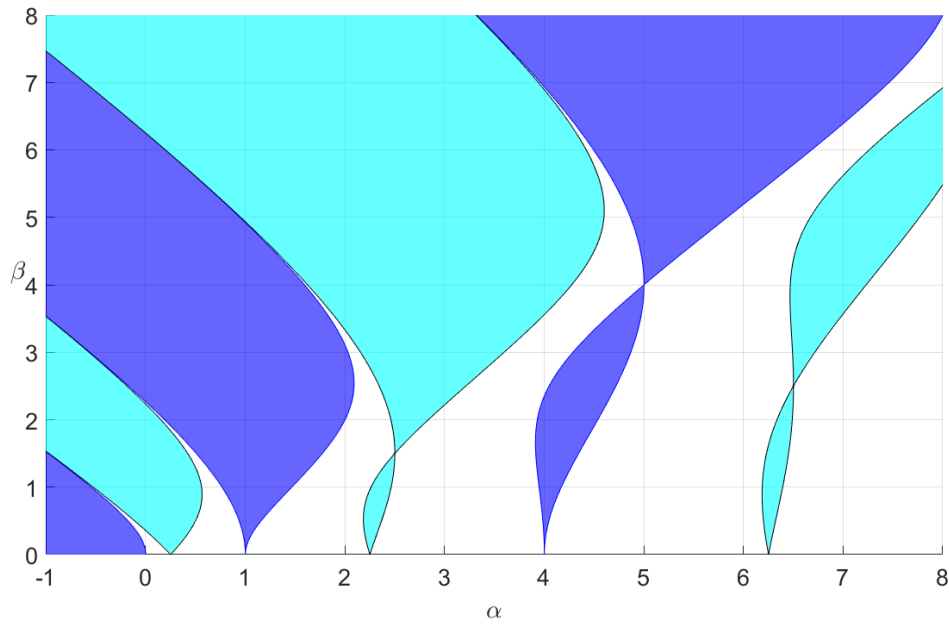


Figure 1.1: Ince-Strutt diagram

An interesting method was the one introduced by Jazar [6]. His approach is applicable to a nonlinear version of the Hill equation. Moreover, his method was also shown to be useful in finding those regions where  $kT$ -periodic solutions exist, for  $k \in \mathbb{N}$ .

For smooth excitation functions, an excellent method, in the sense that it gives accurate results in a very short time, is the one based on spectral differentiation [7]. This method consists in approximating the linear differential operator of Hill equation:

$$\mathcal{L}_H = \frac{d^2}{dt^2} + \beta f(t)$$

through a matrix differential operator which operates on a discrete-time version of a desired solution. This approximation is obtained by globally interpolating a periodic solution  $y(t)$  by means of a band-limited function obtained by the discrete Fourier transform, and then approximating  $\dot{y}$  and  $\ddot{y}$ , respectively, by the first and second derivatives of the interpolant. After obtaining the matrix differential operator approximation, the problem is turned into a periodic *boundary value problem* (BVP), which is solved as the eigenvalue-eigenfunction problem of the matrix operator. Notice that, for the discrete Fourier transform to hold, solution  $y$  should be assumed periodic of some period.

Floquet theory gives a justification of why the Ince-Strutt diagram of the Hill equation can be set as a BVP. In particular, it tells us that a periodic solution of period  $T$  can be found by solving a periodic BVP on the interval  $[0, T]$ , and a periodic solution of period  $2T$  can be found through an anti-periodic BVP on the same interval. These two cases are particular cases of the fact that  $kT$ -periodic and even aperiodic solutions can be found through a twisted BVP [15], which is the generalization of both the periodic and the anti-periodic BVP.

The Sturm-Liouville problem is that formed by the Sturm-Liouville equation:

$$\frac{d}{dt} \left( p(t) \frac{d}{dt} y \right) + q(t)y + \lambda w(t)y = 0,$$

plus some special homogeneous *boundary conditions* (BCs), called the Sturm-Liouville BCs. Its solution are those values of  $\lambda$ , called the eigenvalues of the Sturm-Liouville operator:

$$\mathcal{L} = \frac{1}{w(t)} \left( \frac{d}{dt} \left( p(t) \frac{d}{dt} \right) + q(t) \right),$$

which give rise to non-trivial solutions, called the associated eigenfunctions, that satisfy the Sturm-Liouville BCs.

As the Hill equation is a special case of the Sturm-Liouville equation, for the computation of its Ince-Strutt diagram, the chosen Sturm-Liouville BCs are the periodic and the anti-periodic BCs. For fixed values of  $\beta$ , those values of  $\lambda = \alpha$  inside the transition curves of the Ince-Strutt diagram are computed through both the periodic and the anti-periodic Sturm-Liouville problem, looking for solutions of period  $T$  and  $2T$ , which are the eigenfunctions associated with those values of  $\alpha$ .

The Sturm-Liouville theory gives information about the values of  $\alpha$  inside the transition curves of the Hill equation. These values form a real monotonic sequence,  $\{\alpha_n\}$  for  $n = 0, \dots, \infty$ , which, at the same time, can be decomposed into two disjoint monotonic sequences:  $\{^1\alpha_i\}$  for  $i = 0, \dots, \infty$ , which corresponds to values of  $\alpha$  for which a periodic solution of period  $T$  exist, and  $\{^2\alpha_j\}$  for  $j = 1, \dots, \infty$ , which corresponds to values of  $\alpha$  for which a periodic solution of period  $2T$  exist. By a stability analysis of the Hill equation, it can be proven that the intervals:  $(^1\alpha_j, ^1\alpha_{j+1})$  and  $(^2\alpha_j, ^2\alpha_{j+1})$ , for  $j = 1, \dots, \infty$ , correspond to the instability intervals that form the painted regions in the Ince-Strutt diagram. The coexistence phenomenon arises when an instability interval vanishes, i.e. when  $^1\alpha_j = ^1\alpha_{j+1}$  or  $^2\alpha_j = ^2\alpha_{j+1}$ , which means that two periodic solutions of period  $T$  or  $2T$  *coexist* at the same point in the parameter space. In Figure 1.1, the transition curves of the cyan painted areas correspond to parameters for which  $T$ -periodic solutions exist, whilst the transition

curves of the blue-painted areas correspond to parameters for which  $2T$ -periodic solutions exist.

One of the simplest and fastest methods to find the approximate solution of Sturm-Liouville problems is the one based on finite-differences [8], which has the great disadvantage that only some of the computed eigenvalues are accurate enough to be practical, but has the advantage that it does not require to solve the equation numerically, nor needs to propose a trial function, such as in the shooting method [8] or in variational methods [9]. Approaches that circumvent this obstacle are, for example, the ones in [10] and [11] which consist of approximating the coefficients of the Sturm-Liouville equation by piecewise constant functions and piecewise polynomial functions, respectively, obtaining results with a more uniform estimation error.

For simplicity, a finite-difference scheme for the solution of the twisted Sturm-Liouville problem is chosen, which is reviewed in Chapter 5, and is used in order to find the Ince-Strutt diagram and lines of periodic/aperiodic solutions of various well known special cases of Hill equation, such as Mathieu, Meissner and Lamé equation.

An academic example of a system with periodically varying moment of inertia is given in Chapter 6 to show how this approach can be applied to a slightly more general periodic equation than Hill equation. And finally, an example of application of Mathieu equation is given in Chapter 7.





# Chapter 2

## Background

### 2.1 Floquet Theory

Consider the system of  $n$  linear ordinary differential equations

$$\dot{x} = A(t)x, \quad (2.1)$$

where  $A(t)$  is periodic with minimal period  $T$ , i.e.  $T$  is the minimum positive number such that  $A(t+T) = A(t)$ . These systems will be called *linear periodic systems*.

**Theorem 2.1.1. (Floquet)** [12] *The state transition matrix of a linear periodic system is of the form:*

$$\Phi(t, t_0) = P^{-1}(t)e^{R(t-t_0)}P(t_0), \quad (2.2)$$

where  $P(t) \in \mathbb{R}^{n \times n}$  is periodic of period  $T$ , and  $R \in \mathbb{C}^{n \times n}$  is a constant matrix.

*Proof.* From the periodicity of the state matrix  $A(t)$ , it follows that for every fundamental matrix,  $X(t)$ , there exists a nonsingular matrix,  $M$ , such that  $X(t+T) = X(t)M$ , since  $X(t)$  and  $X(t+T)$  are both fundamental matrices. Then there exists  $R \in \mathbb{C}^{n \times n}$ , called the logarithm of matrix  $M$ , which is not uniquely defined, such that  $M = e^{RT}$ , and so that

$$X(t+T) = X(t)e^{RT} \quad (2.3)$$

Define  $P(t)$  as

$$P(t) = e^{Rt}X^{-1}(t), \quad (2.4)$$

and notice that  $P(t)$  and its inverse (which is defined for all  $t$ ) are periodic with period  $T$ .

Replacing (2.4) in the definition of the state transition matrix one finally gets

$$\begin{aligned}\Phi(t, t_0) &= X(t)X^{-1}(t_0) \\ &= P^{-1}(t)e^{R(t-t_0)}P(t_0)\end{aligned}$$

□

**Theorem 2.1.2.** [5] *System (2.1), has at least one nontrivial complex solution,  $\bar{x}(t)$ , such that*

$$\bar{x}(t+T) = \mu\bar{x}(t), \quad (2.5)$$

where  $\mu$  is a constant.

*Proof.* Let  $X(t)$  be a fundamental matrix of (2.1). Then there exists a nonsingular matrix  $M \in \mathbb{R}^{n \times n}$  such that:  $X(t+T) = X(t)M$ .

Let  $\mu$  be an eigenvalue of  $M$ , and let  $m \in \mathbb{R}^n$  be an associated eigenvector, i.e.:

$$Mm = \mu m \quad (2.6)$$

Consider the solution:  $\bar{x}(t) = X(t)m$ . Then:

$$\begin{aligned}\bar{x}(t+T) &= X(t+T)m \\ &= X(t)Mm \\ &= \mu X(t)m, \text{ (by (2.6))} \\ &= \mu\bar{x}(t)\end{aligned}$$

□

**Theorem 2.1.3.** [5] *Constants  $\mu$  in Theorem 2.1.2 does not depend on the choice of  $X(t)$ .*

*Proof.* Take two fundamental matrices  $X(t)$  and  $\hat{X}(t)$ , and notice that they are related by  $\hat{X}(t) = X(t)C$ , where  $C \in \mathbb{R}^{n \times n}$  is nonsingular since their columns are a basis of the space of solutions. Compute  $\hat{X}(t+T)$ , and you should conclude that all matrices  $M$  that satisfy  $X(t+T) = X(t)M$  for arbitrary  $X(t)$  are similar to each other and thus share the same spectrum. □

After the three theorems above we can now give the following definitions:

**Definition 2.1.1. (Monodromy matrix)** Matrix

$$M = \Phi(T, 0) = e^{RT}, \quad R \in \mathbb{C}^{n \times n} \quad (2.7)$$

where  $\Phi(t, t_0)$  is the state transition matrix of (2.1), is called the monodromy matrix of (2.1).

The monodromy matrix of a system is the standard choice for the construction of the state transition matrix (2.2).

**Definition 2.1.2. (Floquet multipliers)** The eigenvalues,  $\mu$ , of  $M$ , are called the floquet multipliers of system (2.1).

**Definition 2.1.3. (Floquet solution)** A solution  $\bar{x}(t)$  of (2.1) which satisfies (2.5) is called a Floquet solution of (2.1).

**Remark 2.1.1.** If the monodromy matrix  $M$  has  $n$  different eigenvalues, it is straightforward to see that the set of Floquet solutions is linearly independent, and these solutions form a basis of the space of solutions of (2.1). [5]

**Definition 2.1.4. (Floquet exponent)** Consider (2.1). A Floquet exponent  $\rho$  is any complex constant such that

$$\mu = e^{\rho T} \quad (2.8)$$

is a Floquet multiplier of the system.

Floquet exponents  $\rho$  are not uniquely defined, since

$$e^{\rho T} = e^{(\rho + j2\pi m)T}, \quad m \in \mathbb{Z}. \quad (2.9)$$

In particular, if  $T = 2\pi$  and  $\mu$  satisfies:  $\mu = e^{j2\pi\omega}$ , then the Floquet exponents associated with  $\mu$  are:

$$\rho_m = j(\omega + m), \quad m \in \mathbb{Z}. \quad (2.10)$$

For simplicity, it is common to define the Floquet exponent associated with  $\mu$  as:

$$\rho = \frac{1}{T} \ln(\mu)$$

taking the principal value of  $\ln(\cdot)$ .

**Remark 2.1.2.** *Choosing  $X(t) = \Phi(t, 0)$  in (2.4), we have that  $e^{RT} = \Phi(T, 0) = M$  is the monodromy matrix of the system. Then, from matrix function theory, Floquet exponents are no others but the eigenvalues of the chosen  $R$ .*

The previous Remark implies that matrix  $R$  is defined by the choice of Floquet exponents or vice versa.

To conclude this section, the next theorem is a version of Theorem 2.1.2 in terms of the previous definitions. The importance of this Theorem lies in the fact that it sets the problem of finding Floquet solutions of a  $T$ -periodic system as a BVP.

**Theorem 2.1.4.** *[15] Let  $M$  be the monodromy matrix of the  $T$ -periodic system (2.1), and let  $\mu \in \mathbb{C}$ . Then  $\mu$  is a Floquet multiplier of  $M$  if and only if there is a non-trivial (in general complex) solution  $\bar{x}$  such that  $\bar{x}(T) = \mu\bar{x}(0)$ .*

*Proof.* Suppose  $M$  is the monodromy matrix of the system, and that  $\mu$  is a Floquet multiplier, then if  $\bar{x}(0)$  is chosen as the eigenvector associated with  $\mu$ , we have that  $\bar{x}(T) = M\bar{x}(0) = \mu\bar{x}(0)$ . Conversely, if  $\bar{x}(t)$  is a nontrivial solution satisfying  $\bar{x}(T) = \mu\bar{x}(0)$  then  $\bar{x}(0)$  is an eigenvector of  $M$  associated with the eigenvalue  $\mu$ , since it satisfies:

$$\bar{x}(T) = M\bar{x}(0) = \mu\bar{x}(0).$$

□

## 2.2 Linear Hamiltonian systems

**Definition 2.2.1.** *A matrix  $A \in \mathbb{R}^{2n \times 2n}$  is called Hamiltonian if it satisfies*

$$A^T J + JA = 0, \quad J = \begin{bmatrix} 0 & I \\ -I & 0 \end{bmatrix} \quad (2.11)$$

A linear system

$$\dot{x} = A(t)x \quad (2.12)$$

is called a *linear Hamiltonian* system if its state matrix  $A(t)$  is a Hamiltonian matrix.

Consider

$$A = \begin{bmatrix} a & b \\ c & d \end{bmatrix} \quad (2.13)$$

where  $a, b, c, d \in \mathbb{R}^{n \times n}$ . Then, by (2.11), it is easy to see that  $A$  is Hamiltonian if and only if  $a^T + d = 0$  and  $b$  and  $c$  are symmetric. In the  $2 \times 2$  case, a matrix is Hamiltonian if and only if its trace is zero. In the context of dynamical systems, a second order 1-DOF linear system is then Hamiltonian whenever dissipation terms are being neglected.

**Theorem 2.2.1.** *Let  $A$  be Hamiltonian. If  $\rho \in \sigma(A)$ , then  $-\rho \in \sigma(A)$ .*

*Proof.* Notice  $J$  is orthogonal, i.e.  $J^{-1} = J^T$ . Rearranging (2.11) we get

$$JAJ^T = -A^T,$$

then  $A$  is similar to  $-A^T$ . Finally, since the spectrum of  $-A$  equals the spectrum of  $-A^T$ , we have  $\sigma(A) = \sigma(-A)$   $\square$

**Definition 2.2.2.** *A matrix  $M \in \mathbb{R}^{2n \times 2n}$  is called  $\gamma$ -symplectic if it satisfies*

$$M^T J M = \gamma J. \quad (2.14)$$

with constant  $\gamma \neq 0$ . If  $\gamma = 1$ , then  $M$  is called symplectic.

Consider again (2.13), and take  $M = A$ , then it is easy to see that  $M$  is  $\gamma$ -symplectic if and only if  $a^T d - c^T b = \gamma I$  and  $a^T c$  and  $b^T d$  are symmetric. In the  $2 \times 2$  case, this condition becomes simply  $\det(M) = \gamma$ .

**Theorem 2.2.2.** *Let  $M$  be  $\gamma$ -symplectic. If  $\mu \in \sigma(M)$  then  $\gamma/\mu \in \sigma(M)$ .*

*Proof.* Since  $\det(M) = \gamma$ ,  $\gamma \neq 0$ , there exists  $M^{-1}$ . Then, from (2.14), we have

$$J^T M^T J = \gamma M^{-1},$$

which implies  $\sigma(M) = \delta \sigma(M^{-1})$ .  $\square$

For a  $\gamma$ -symplectic matrix  $M \in \mathbb{R}^{2n}$ , the Theorem 2.2.2 implies that its eigenvalues,  $\mu_1, \mu_2$ , must either be complex conjugates and lie on the circle of radius  $\sqrt{\delta}$ , or be both real and such that  $\mu_1 = \gamma/\mu_2$ .

The set  $Sp(2n, \mathbb{R})$  of symplectic matrices is a subgroup of  $Gl(2n, \mathbb{R})$ , the group of non-singular matrices under matrix multiplication. This means, in particular, that the product of any two symplectic matrices is symplectic.

Now, next Theorem relates Hamiltonian systems with symplectic matrices.

**Theorem 2.2.3.** *[16] The state transition matrix  $\Phi(t, t_0)$  of a linear Hamiltonian system is symplectic  $\forall t, t_0 \in \mathbb{R}$ . Conversely, if  $\Phi(t, t_0)$  is a continuously differentiable symplectic matrix, then it is a state transition matrix of a linear Hamiltonian system.*

*Proof.* Let  $\Phi(t, t_0)$  be the state transition matrix of (2.12), then  $\Phi(t_0, t_0) = I$ , which implies  $\Phi^T(t, t_0)J\Phi(t, t_0) = J$  at  $t = t_0$ . Derivation with respect to time yields

$$\frac{d}{dt} (\Phi^T(t, t_0)J\Phi(t, t_0)) = \Phi^T(t, t_0) (A^T J + JA) \Phi(t, t_0) = 0$$

since  $A^T J + JA = 0$  for  $A$  being Hamiltonian. Then  $\Phi^T(t, t_0)J\Phi(t, t_0) = J \quad \forall t, t_0 \in \mathbb{R}$ .

For the second part, notice  $A = \dot{\Phi}(t, t_0)\Phi^{-1}(t, t_0)$  is Hamiltonian and  $\dot{\Phi}(t, t_0) = A\Phi(t, t_0)$ . □

## 2.3 Reducibility

A linear time-varying system

$$\dot{x} = A(t)x \tag{2.15}$$

is said to be algebraically equivalent to the alternative linear time-varying system

$$\dot{z} = \bar{A}(t)z \tag{2.16}$$

if there exist a non-singular continuously differentiable matrix  $P(t)$ , called an equivalence transformation, such that  $x = P(t)z$ . Nevertheless, contrary to the time-invariant case, stability properties are not preserved under equivalence transformation. In fact, any time-varying linear system can be shown to be algebraically equivalent to a system with state matrix  $\bar{A}$ , where  $\bar{A}$  is a constant arbitrary matrix. In particular, any time-varying system is algebraically equivalent to a system with state matrix  $\bar{A} = 0$ . To circumvent this obstacle, we can restrict ourselves to a special kind of transformation:

**Definition 2.3.1. (Lyapunov transformation)** A  $n$  by  $n$  matrix  $P(t)$  is called a Lyapunov transformation if:

- $P(t)$  is non-singular on  $\mathbb{R}$
- $P(t)$  and  $\dot{P}(t)$  are continuous on  $\mathbb{R}$ .
- $P(t)$  and  $P^{-1}$  are bounded on  $\mathbb{R}$

**Definition 2.3.2.** Two systems (2.15) and (2.16) are said to be Lyapunov equivalent if they are algebraically equivalent under a Lyapunov transformation.

Before we introduce the definition of reducible systems, let us see that stability properties are preserved under Lyapunov transformations.

**Theorem 2.3.1.** *Suppose systems (2.15) and (2.16) are Lyapunov equivalent under the Lyapunov transformation  $P(t)$ , then system (2.15) is uniformly (exponentially) stable if and only if (2.16) is uniformly (exponentially) stable.*

*Proof.* Suppose  $\Phi_x(t, t_0)$  and  $\Phi_z(t, t_0)$  are, respectively, the state transition matrices of systems (2.15) and (2.16). Then it can be noticed that they are related by:

$$\Phi_x(t, t_0) = P^{-1}(t)\Phi_z(t, t_0)P(t_0)$$

and the rest of the proof follows easily from the fact that  $P(t)$  and  $P^{-1}(t)$  are bounded, see [13].  $\square$

**Definition 2.3.3.** *A time-varying linear system is called reducible, in the sense of Lyapunov, if it is Lyapunov equivalent to a linear system with a constant state matrix.*

And finally, returning to linear periodic systems:

**Theorem 2.3.2.** *The linear periodic system (2.1) is reducible in the sense of Lyapunov.*

*Proof.* Start by noticing that  $e^{Rt}$  in (2.2) can be regarded as the state transition matrix of the linear system with constant state matrix

$$\dot{z} = Rz. \tag{2.17}$$

Choose  $z = P(t)x$ , then

$$\begin{aligned} \dot{z} &= \dot{P}(t)x + P(t)\dot{x} \\ &= \dot{P}(t)x + P(t)A(t)x \\ &= (\dot{P}(t) + P(t)A(t))P^{-1}(t)z \end{aligned}$$

Notice

$$\begin{aligned} \dot{P}(t) &= Re^{Rt}\Phi^{-1}(t, 0) + e^{Rt}\dot{\Phi}^{-1}(t, 0) \\ &= Re^{Rt}\Phi^{-1}(t, 0) - e^{Rt}\Phi^{-1}(t, 0)\dot{\Phi}(t, 0)\Phi^{-1}(t, 0) \\ &= RP(t) - P(t)A(t) \end{aligned}$$

Replacing, we finally obtain

$$\begin{aligned}\dot{z} &= (\dot{P}(t) + P(t)A(t))P^{-1}z \\ &= (RP(t) - P(t)A(t) + P(t)A(t))P^{-1}z \\ &= Rz\end{aligned}$$

Now there is only left to prove  $P(t)$  is also a Lyapunov transformation.

Remember that, in this case,  $P(t)$  and  $P^{-1}(t)$  are periodic with period  $T$ , so it is only necessary to analyze these matrices over the interval  $[0, T]$ . For simplicity, choose  $X(t) = \Phi(t, 0)$  in (2.4), then

$$P(t) = e^{Rt}\Phi^{-1}(t, 0)$$

For a bounded piece-wise continuous state matrix  $A(t)$  it can be proved that the correspondent state transition matrix,  $\Phi(t, t_0)$ , is continuous, invertible for all  $t, \tau \in \mathbb{R}$ , and bounded on every finite interval, which implies

$$P^{-1}(t) = \Phi(t, 0)e^{-Rt}$$

is bounded and continuous. □

Finally, it is important to point out that, in fact, *Lyapunov equivalence* is an equivalence relation. This can be easily seen after verifying that if  $P_1$  and  $P_2$  are Lyapunov transformations, then  $P_1P_2$  is also a Lyapunov transformation.



# Chapter 3

## Hill equation

Consider  $x = [y, \dot{y}]^T$ , then Hill equation (1.1) can be rewritten as follows:

$$\dot{x} = A(t)x \quad (3.1)$$

with

$$A(t) = \begin{bmatrix} 0 & 1 \\ -h(t) & 0 \end{bmatrix} \quad (3.2)$$

where  $h(t)$  is periodic with minimal period  $T > 0$ .

When damping is considered, (1.1) becomes

$$\ddot{y} + \delta \dot{y} + h(t)y = 0 \quad (3.3)$$

where  $\delta > 0$ . Choosing again  $x = [y, \dot{y}]^T$ , we obtain in this case

$$A(t) = \begin{bmatrix} 0 & 1 \\ -h(t) & -\delta \end{bmatrix}. \quad (3.4)$$

### 3.1 Preliminaries

Let us start by noticing every linear second order equation

$$a_0(t)\ddot{z} + a_1(t)\dot{z} + a_2(t)z = 0 \quad (3.5)$$

with  $a_0(t) > 0$ , can be transformed into the form:

$$\ddot{y} + q(t)y = 0 \quad (3.6)$$

by the change of variable

$$z = y \exp\left(-\frac{1}{2} \int^t \frac{a_1(\tau)}{a_0(\tau)} d\tau\right) \quad (3.7)$$

where

$$q(t) = \frac{a_2(t)}{a_0(t)} - \frac{1}{4} \left(\frac{a_1(t)}{a_0(t)}\right)^2 - \frac{1}{2} \frac{d}{dt} \left(\frac{a_1(t)}{a_0(t)}\right)$$

Transformation (3.6) is useful if the objective is to analyze the zeros of the solutions  $z(t)$  of (3.5). But it does not, in general, induce a Lyapunov transformation, i.e. it does not, in general, preserve stability properties. For example, it could happen that the dynamics of variable  $y$  is stable, but the dynamics of variable  $z$  is unstable due to the exponential term in (3.7). However, if coefficients  $a_i(t)$  are restricted to be periodic with common period  $T$ , then (3.5) is Lyapunov equivalent to the damped Hill equation (3.3), as we are about to prove.

Consider (3.5) with  $a_1(t)/a_0(t)$  bounded, periodic with period  $T$ , and continuously differentiable. First, let us prove that  $a_1(t)/a_0(t)$  can be decomposed as the sum of a zero mean value periodic solution plus a constant. Define  $h$  as

$$h(t) = \int^t \frac{a_1(\tau)}{a_0(\tau)} d\tau,$$

then

$$h(t+T) - h(t) = \int_x^{x+T} \frac{a_1(\tau)}{a_0(\tau)} d\tau = c$$

for some constant  $c$ , since  $a_1(t)/a_0(t)$  is periodic.

Now define  $g(t) = a_1(t)/a_0(t) - c/T$ . Then

$$g(t+T) - g(t) = \int_x^{x+T} \frac{a_1(\tau)}{a_0(\tau)} d\tau - c = 0, \forall t.$$

which means that  $g(t)$  is periodic with period  $T$ .

From the previous discussion, we can rewrite (3.5) as

$$\ddot{z} + \left( \dot{h}(t) + \frac{c}{T} \right) \dot{z} + \frac{a_2(t)}{a_0(t)} z = 0 \quad (3.8)$$

Now consider the transformation

$$z = y \exp(-(1/2)g(t)). \quad (3.9)$$

Since  $g(t)$  is periodic, bounded and differentiable, then  $e^{-(1/2)g(t)}$  and its inverse are bounded and differentiable, so transformation (3.9) gives rise to the Lyapunov transformation

$$\begin{bmatrix} z \\ \dot{z} \end{bmatrix} = P(t) \begin{bmatrix} y \\ \dot{y} \end{bmatrix} \quad (3.10)$$

where

$$P(t) = e^{-\frac{1}{2}g(t)} \begin{bmatrix} 1 & 0 \\ -\frac{1}{2}\dot{g}(t) & 1 \end{bmatrix} \quad (3.11)$$

Applying this transformation to (3.8), and defining  $\delta = c/T$ , we obtain the equivalent system

$$\ddot{y} + \delta \dot{y} + q(t)y = 0 \quad (3.12)$$

where

$$q(t) = \left( \frac{a_2(t)}{a_0(t)} - \frac{\delta}{2}\dot{g}(t) - \frac{1}{4}|\dot{g}(t)|^2 - \frac{1}{2}\ddot{g}(t) \right) \quad (3.13)$$

Notice that, since  $g(t)$  is periodic with period  $T$ , then (3.13) is also periodic with the same period, and so (3.12) is in the form of the damped Hill equation (3.3).

In conclusion, under some restrictions, an equation (3.5), with periodic coefficients, is Lyapunov equivalent to the damped Hill equation, where the mean value of the coefficient  $a_1(t)/a_0(t)$ , if positive, acts as a damping coefficient, and, if negative, acts as a driving coefficient. The case where  $a_1(t)/a_0(t)$  has zero mean value is the case when transformation (3.9) equals transformation (3.7), and it induces the Lyapunov transformation (3.10).

## 3.2 Periodic and aperiodic solutions

Let us start by mentioning that, contrary to the intuition, solutions of linear periodic systems are not in general periodic. For example, take the one dimensional system

$$\dot{x} = \alpha + \sin(t)x$$

whose general solution is of the form:

$$x(t) = c_1 e^{\alpha t - \cos(t)}.$$

Periodic solutions appear only if  $\alpha = 0$ .

Consider the linear periodic system (2.1) with monodromy matrix  $M$ . By (2.3), its state transition matrix satisfies:

$$\Phi(t+T, t_0+T) = \Phi(t, t_0). \quad (3.14)$$

Then  $\Phi(kT, 0) = \Phi^k(T, 0) = M^k$ .

Now suppose that  $x(t)$  is a solution of (2.1). Then  $x(t+kT)$  can be expressed as:

$$\begin{aligned} x(t+kT) &= \Phi(t+kT, 0)x(0), \\ &= \Phi(t, 0)M^k x(0). \end{aligned} \quad (3.15)$$

If  $x(t)$  is a Floquet solution of (2.1), then (3.15) reduces to:

$$x(t+kT) = \mu^k x(t). \quad (3.16)$$

If  $\mu$  happens to be a  $k$ th unity-root, i.e.  $\mu$  satisfies:  $\mu^k - 1 = 0$ , then  $x(t+kT) = x(t) \forall t \in \mathbb{R}$ , and the Floquet solution is periodic with period  $kT$ , although it might not be its minimum period.

**Definition 3.2.1.** We say that  $\mu$  is a primitive  $k$ th unity-root if it satisfies  $\mu^k - 1 = 0$  and  $\mu^m - 1 \neq 0 \forall m < k$ , with  $m, k \in \mathbb{N}$ .

In other words, a unity-root is a *primitive  $k$ th unity-root* if it is a  $k$ th unity-root and not a  $m$ th unity-root for any natural number  $m$  smaller than  $k$ .

**Remark 3.2.1.** If  $\mu$  is a unity-root, then so is  $\mu^*$ , since they are roots of a polynomial with real coefficients.

In polar form,  $k$ th unity-roots can be set as:

$$\mu_p = e^{j2\pi\frac{p}{k}}, p \in \{0, 1, \dots, k-1\}, k \in \mathbb{N} \quad (3.17)$$

noticing this is not a unique representation, because  $\mu_p = e^{j2\pi\frac{p}{k}} = e^{j2\pi(\frac{p}{k}+q)}$  as  $e^{j2\pi q} = 1 \forall q \in \mathbb{Z}$ .

**Remark 3.2.2.** A complex number (3.17) is a primitive  $k$ th unity-root if and only if  $p$  and  $k$  are coprime integers (i.e.  $p/k$  is an irreducible fraction). For example:  $e^{j2\pi/8}$  and  $e^{j2\pi(3/8)}$  are primitive 8th unity-roots, while  $e^{j2\pi(2/8)}$  is not, since  $2/8 = 1/4$  and thus is also a 4th unity-root.

**Lemma 3.2.1.** Consider the Hill equation:

$$\ddot{y} + h(t)y = 0, \quad (3.18)$$

where  $h$  is periodic with minimal period  $T > 0$  and  $h \in \mathbb{C}^0$ . If  $\phi$  is a non-trivial periodic solution of (3.18), then its minimal period must be a multiple of  $T$ .

*Proof.* Suppose  $\phi$  is a non-trivial periodic solution of (3.18) with minimal period  $aT$ ,  $a \in \mathbb{R}$ . It will be proven that  $a$  must, in fact, be an integer.

As  $\phi(t)$  it is a solution, then it satisfies:

$$\ddot{\phi}(t) + h(t)\phi(t) = 0, \forall t \in \mathbb{R}, \quad (3.19)$$

but because (3.19) holds  $\forall t$ , then, in particular

$$\ddot{\phi}(t + aT) + h(t + aT)\phi(t + aT) = 0, \forall t \in \mathbb{R} \quad (3.20)$$

By the definition of the derivative of a function and the periodicity of  $\phi(t)$ , it is easy to prove that  $\dot{\phi}(t + aT) = \dot{\phi}(t)$  and  $\ddot{\phi}(t + aT) = \ddot{\phi}(t)$ , so (3.20) implies:

$$\ddot{\phi}(t) + h(t + aT)\phi(t) = 0, \forall t \in \mathbb{R} \quad (3.21)$$

Subtracting (3.19) from (3.21) we have:

$$(h(t + aT) - h(t))\phi(t) = 0, \forall t \in \mathbb{R} \quad (3.22)$$

Observe that  $\phi(t)$  has zeros only at isolated values of  $t$ , since if it weren't true, then there would exist an interval  $J$  in which  $\phi(t) = 0$  and  $\dot{\phi}(t) = 0$ ,  $\forall t \in J$ , which would imply, by

uniqueness of solutions, that  $\phi(t) = 0 \forall t \in \mathbb{R}$ , which is a contradiction since we regarded it as nontrivial. Then, by the continuity of  $h$ ,  $h(t + aT) = h(t) \forall t \in \mathbb{R}$ , which finally implies  $a \in \mathbb{Z}$ , since  $T$  is the minimal period of  $h(t)$ . □

**Remark 3.2.3.** Condition  $h(t) \in \mathbb{C}^0$  in the previous Lemma can be replaced by the weaker condition:  $h \in \mathbb{P}\mathbb{C}^0$  and  $h(t + aT) = h(t) \implies a \in \mathbb{Z}$ , where  $\mathbb{P}\mathbb{C}^0$  is the set of piece-wise continuous functions on  $\mathbb{R}$ .

**Corollary 3.2.1.** (To Theorem 2.1.4)

Consider the  $T$ -periodic Hill equation (3.1). Let  $M$  be its monodromy matrix with Floquet multipliers  $\mu_1 = \mu_2^*$ .

- **a)** If and only if Floquet multipliers are primitive  $k$ th unity-roots for  $k \geq 3$ , then all the solutions are periodic with minimal period  $kT$ .
- **b)** If and only if Floquet multipliers are primitive  $k$ th unity-roots with  $k \in \{1, 2\}$ , there exist at least one solution, unique up to a scale factor, with minimal period  $kT$ .

*Proof.* **a)** Start by supposing  $\mu_1, \mu_2$  are primitive  $k$ th unity-roots such that  $k \geq 3$ , then  $\mu_1 \neq \mu_2$ , so

$$M = Q \begin{bmatrix} \mu_1 & 0 \\ 0 & \mu_2 \end{bmatrix} Q^{-1}$$

which implies

$$M^k = Q \begin{bmatrix} \mu_1^k & 0 \\ 0 & \mu_2^k \end{bmatrix} Q^{-1} = I$$

Then, for an arbitrary initial condition  $x(0) = x_0 \in \mathbb{R}^2$ , the general solution of system (3.1) satisfies

$$\begin{aligned} x(t + kT) &= \Phi(t + kT, 0)x_0 \\ &= \Phi(t + kT, T)Mx_0 \\ &= \Phi(t + (k - 1)T, 0)Mx_0 \\ &\vdots \\ &= \Phi(t, 0)M^k x_0 \\ &= \Phi(t, 0)x_0 = x(t) \end{aligned}$$

Minimality of the period of the general solution  $x(t)$  is ensured by Lemma 1, since it holds that  $M^k = I$ ,  $M^m \neq I$ , for  $m < k$ ,  $m, k \in \mathbb{N}$ .

For the converse, suppose all solutions of (3.1) are periodic with minimal period  $kT$ , then any solution  $x(t)$  with arbitrary initial condition  $x(0) = x_0 \in \mathbb{C}$  satisfies

$$x(t + kT) = \Phi(t, 0)M^k x_0 = \Phi(t, 0)x_0 \quad (3.23)$$

so  $M^k = I$  which implies  $\mu_1^k = \mu_2^k = 1$ . Notice that minimality of  $k$  is ensured by the fact that  $kT$  is the minimal period of  $x(t)$ , and then the Floquet multipliers are primitive  $k$ th unity-roots.

**b)** Suppose now that  $\mu_1$  and  $\mu_2$  are primitive  $k$ th unity-roots where  $k \in \{1, 2\}$ . In both cases we have  $\mu_1 = \mu_2$ , then, in general:

$$M = Q \begin{bmatrix} \mu_1 & 1 \\ 0 & \mu_2 \end{bmatrix} Q^{-1}$$

and so

$$\begin{aligned} M^k &= Q \begin{bmatrix} \mu_1^k & k \\ 0 & \mu_2^k \end{bmatrix} Q^{-1} \\ &= Q \begin{bmatrix} 1 & k \\ 0 & 1 \end{bmatrix} Q^{-1} \end{aligned}$$

If we choose  $x(0) = x_0$  as an eigenvector of  $M^k$  associated with  $\mu^k = 1$ , then

$$\begin{aligned} x(t + kT) &= \Phi(t, 0)M^k x_0 \\ &= \Phi(t, 0)x_0 = x(t). \end{aligned}$$

Again, minimality of the period of the solution  $x(t)$  is ensured by Lemma 1.

For the converse, suppose there exist a periodic solution  $x(t)$ , with minimal period  $kT$  and initial condition  $x_0$ , such that

$$x(t + kT) = \Phi(t, 0)M^k x_0 = \Phi(t, 0)x_0$$

then  $1 \in \sigma(M^k)$  and  $x_0$  is one of its associated eigenvectors. Since  $\mu_1^k = (\mu_2^*)^k$ , then  $\mu_1^k = \mu_2^k = 1$ . Again, minimality of  $k$  is ensured by the fact that  $kT$  is the minimal period of  $x(t)$ , and then the Floquet multipliers are  $k$ th unity-roots. □

### 3.3 Stability

Let us start by decomposing the time variable  $t$  as

$$t = \tau + kT, \quad k \in \mathbb{Z}, \quad \tau \in [0, T). \quad (3.24)$$

Then the general solution of (3.1) can be set as:

$$x(t) = x(\tau + kT) = \Phi(\tau, 0)M^k x(0) \quad (3.25)$$

Notice that, for state matrix,  $A(t)$ , bounded, the state transition matrix  $\Phi(t, t_0)$  is bounded on a finite interval ([12], [14]), then boundedness of solutions of (3.1) depend exclusively on  $M$ , in particular, on its eigenvalues.

From (3.24),  $t \rightarrow \infty \iff k \rightarrow \infty$ . Next, as  $\Phi(\tau, 0)$  is bounded for  $\tau \in [0, T)$ , for stability purposes, we analyze only the case where  $\tau = 0$ . Then boundedness of the solutions of the linear periodic system (3.1) is *equivalent* to boundedness of the solutions of the discrete-time system:

$$x_{k+1} = Mx_k, \quad (3.26)$$

whose general solution is:

$$x_k = M^k x_0, \quad (3.27)$$

where  $x_k = x(kT)$ .

From the previous discussion, the trivial solution of (3.1) is:

- asymptotically stable  $\iff \sigma(M) \subset \overset{\circ}{D} \triangleq \{s \in \mathbb{C} : |s| < 1\}$ .
- stable  $\iff \sigma(M) \subset \bar{D} \triangleq \{s \in \mathbb{C} : |s| \leq 1\}$ , and every  $\mu \in \sigma(M)$  such that  $|\mu| = 1$ , is a simple root of the minimal polynomial of  $M$ .
- unstable  $\iff$  exists at least one  $\mu \in \sigma(M)$  such that either  $|\mu| > 1$  or  $|\mu| = 1$  and is a multiple root of the minimal polynomial of  $M$ .



Now, since system (3.1) is linear hamiltonian, its state transition matrix is symplectic, i.e.  $\det(M) = \mu_1\mu_2 = 1$ . Thus the characteristic equation of  $M$  is:

$$\mu^2 - \text{tr}(M) + 1 = 0 \quad (3.28)$$

whose roots are

$$\mu_{1,2} = \frac{\text{tr}(M) \pm \sqrt{|\text{tr}(M)|^2 - 4}}{2} \quad (3.29)$$

Finally, from (3.29) we can see that the stability of (3.1) depends on the values of  $\text{tr}(M)$ , where we distinguish three cases:

- For  $|\text{tr}(M)| = 2$ , we are at the boundary case where the Floquet multipliers are  $\mu_1 = \mu_2 = \pm 1$ , i.e. are real and repeated on the unit circle, then solutions are in general unbounded.
- For  $|\text{tr}(M)| < 2$ , Floquet multipliers are different, complex conjugate, and lie on the unit circle, then solutions are bounded.
- For  $|\text{tr}(M)| > 2$ , Floquet multipliers are different, real, and  $|\mu_1| < 1 \implies |\mu_2| > 1$  since  $\mu_1\mu_2 = 1$ , then solutions are unbounded.

These three cases mean that solutions can either be bounded or unbounded. Asymptotic stability cannot occur for the Hill equation (3.1).

Notice from the definition of  $M$  that  $\text{tr}(M) = y_1(T) + \dot{y}_2(T)$ , where  $y_1(t), y_2(t)$  are the solutions of (1.1) that satisfy the initial conditions:  $y_1(0) = 1, \dot{y}_1(0) = 0, y_2(0) = 0, \dot{y}_2(0) = 1$ . If we consider the vector of parameters  $p$  for the Hill equation, from the theorem of continuity with respect to parameters [19], we can take  $\text{tr}(M) = \text{fun}(p)$ , where  $\text{fun}(p)$  is a function that varies continuously with respect to continuous changes in the parameters  $p$ .

The case of our interest will be  $|\text{tr}(M)| = 2$ , or equivalently,  $\mu_1 = \mu_2 = \pm 1$ . Notice that  $\mu = 1 = e^{j2\pi}$  and  $\mu = -1 = e^{j2\pi\frac{1}{2}}$ , then, by the theory presented in the previous section, finding the regions in the parameter space where periodic solutions of minimal period  $T$  or  $2T$  exist, means finding the transition curves of the Ince-Strutt diagram of the Hill equation.

### 3.3.1 Damping

Consider the damped Hill equation (3.3). In state space form, with state variable  $x = [y, \dot{y}]$ , its state matrix is (3.4).

The system defined by (3.3) and the state matrix (3.4) is not linear Hamiltonian. Nevertheless, by the Jacobi-Liouville-Abel Theorem [13], it can be proven that the monodromy matrix  $M$  of (3.3) satisfies

$$\det(M) = e^{-\delta T} = \gamma$$

which implies that  $M$  is  $\gamma$ -symplectic. Since  $\delta > 0$ , then  $\gamma < 1$ , and the Floquet multipliers of (3.3) may lie inside the unit circle. This means that, contrary to the undamped case, asymptotic stability is possible. To prove this, notice that the characteristic polynomial of  $M$  is

$$\mu^2 - \operatorname{tr}(M)\mu + \gamma = 0$$

which implies

$$\mu_{1,2} = \frac{\operatorname{tr}(M) \pm \sqrt{|\operatorname{tr}(M)|^2 - 4\gamma}}{2}$$

### 3.4 Reducibility

In section (2.1) it was mentioned that the Floquet exponents of an linear periodic system (2.1) are the eigenvalues of a matrix  $R \in \mathbb{C}^{n \times n}$  in (2.2). This is because the matrix natural logarithm is not unique, even in the real case, since  $I = e^0 = e^{2\pi J}$ , where

$$J = \begin{bmatrix} 0 & 1 \\ -1 & 0 \end{bmatrix}$$

Take  $T = 2\pi$  and let  $M$  be the monodromy matrix of (3.1). Let  $\mu_1, \mu_2^*$  be the Floquet exponents of the system. If, for simplicity, we take  $\mu_1 \neq \mu_2$ , then, from (2.7), we can define  $R$  such that

$$\sigma(R) = \{\ln(\mu_1), \ln(\mu_2)\} = \{\rho_1, \rho_2\}$$

taking  $\rho_i$  as the principal value of  $\ln(\mu_i)$ .

Since  $M$  is symplectic,  $\mu_1 = 1/\mu_2$ , and  $\rho_1 = -\rho_2$ . We can distinguish two interesting cases:

Suppose that the Floquet multipliers of the system lie on the unit circle and are such that the Floquet exponents can be chosen as  $\rho_{1,2} = \pm j\omega$ ,  $\omega \in (0, \pi)$ . Then matrix  $R$  from (2.7)

is chosen as

$$R = Q^{-1} \begin{bmatrix} 0 & \omega \\ -\omega & 0 \end{bmatrix} Q$$

and the Monodromy matrix of the system can be set as

$$\begin{aligned} M = e^{2\pi R} &= Q^{-1} \exp \left( 2\pi \begin{bmatrix} 0 & \omega \\ -\omega & 0 \end{bmatrix} \right) Q, \\ &= Q^{-1} \exp \left( 2\pi \begin{bmatrix} 0 & \omega \\ -\omega & 0 \end{bmatrix} + 2\pi m \begin{bmatrix} 0 & 1 \\ -1 & 0 \end{bmatrix} \right) Q, \quad m \in \mathbb{Z} \\ &= Q^{-1} \exp \left( 2\pi \begin{bmatrix} 0 & \omega + m \\ -(\omega + m) & 0 \end{bmatrix} \right) Q \end{aligned}$$

since

$$e^C = e^{C+2\pi J}$$

for any matrix  $C \in \mathbb{C}^{2 \times 2}$ , and

$$J = \begin{bmatrix} 0 & 1 \\ -1 & 0 \end{bmatrix}$$

The previous discussion implies that (3.1) is Lyapunov equivalent to not only a particular  $R$ , but to an infinite set of matrices  $\{R_m\}$ , given by

$$R_m = Q^{-1} \begin{bmatrix} 0 & \omega + m \\ -(\omega + m) & 0 \end{bmatrix} Q, \quad m \in \mathbb{Z}$$

Notice that matrices  $R_m$  are equivalent to harmonic oscillators with natural frequencies from the set  $\{\omega_m \mid \omega_m = \omega + m, m \in \mathbb{Z}\}$ . Moreover, by transitivity, the Hill equation is Lyapunov equivalent to an infinite set of harmonic oscillators.

If  $\mu_1, \mu_2$  lie off the unit circle, then we can set  $\rho_1 = \rho \in \mathbb{R}, \rho \neq 0$ , and

$$R = Q^{-1} \begin{bmatrix} \rho & 0 \\ 0 & -\rho \end{bmatrix} Q$$

which means that the Hill equation is, in this case, Lyapunov equivalent to a linear system with a saddle instability at the trivial solution.

## 3.5 Coexistence

Consider Hill equation. According to Corollary 3.2.1, if Floquet multipliers are  $\mu_{1,2} = 1$  (respectively,  $\mu_{1,2} = -1$ ), then, in general, there will be only one linearly independent  $T$ -periodic solution (respectively,  $2T$ -periodic solution), since the Jordan form of the monodromy matrix  $M$  (respectively,  $M^2$ ) is, in general, triangular. Whenever two linearly independent  $T$ -periodic ( $2T$ -periodic) solutions exist for a certain point  $(\alpha, \beta)$  in the parameter space, then these two solutions are said to coexist, and we will say that  $(\alpha, \beta)$  is a point of coexistence.

### 3.5.1 Lamé equation

The Lamé equation is a particular case of the Hill equation:

$$\ddot{y} + (\alpha + \beta(\beta + 1)\gamma \operatorname{sn}^2(t))y = 0 \quad (3.30)$$

where  $\operatorname{sn}(t)$  is a Jacobi elliptic function, and  $\gamma$  is its modulus [17]. For  $t \in \mathbb{R}$ , function  $\operatorname{sn}(t)$  is periodic with period  $2K$ , where

$$K = \int_0^{\pi/2} \frac{d\tau}{\sqrt{1 - \gamma \sin^2(\tau)}}$$

The interesting phenomenon that appears in the Lamé equation is summarized in the following Theorem:

**Theorem 3.5.1.** [1] *If and only if  $\beta$  is an integer can periodic solutions of period  $2K$  or  $4K$  in the Lamé equation coexist. If  $m$  is defined by  $m = \beta$  when  $\beta$  is a non-negative integer and by  $m = -\beta - 1$  when  $\beta$  is a negative integer, then Lamé equation will have at most  $m + 1$  intervals of instability, including the zeroth interval which starts at  $\alpha = -\infty$ .*

The proof of this theorem can be found on [1]. In summary, Theorem 3.5.1 says that the Lamé equation has only a finite number of instability intervals for integer values of  $\beta$ .

# Chapter 4

## Sturm-Liouville theory

This section summarizes important facts and results on Sturm-Liouville theory, which can be applied to the problem of finding the Ince-Strutt diagram of the Hill equation.

### 4.1 Sturm-Liouville equation

The self-adjoint equation:

$$\frac{d}{dt} \left( p(t) \frac{dy}{dt} \right) + q(t)y + \lambda w(t)y = 0, \quad (4.1)$$

defined on an interval  $[a, b]$ , is called the Sturm-Liouville equation if

- $p(t)$ ,  $\dot{p}(t)$ ,  $q(t)$ ,  $w(t)$  are real and continuous on  $[a, b]$ .
- $p(t) > 0$  and  $w(t) > 0$  on  $[a, b]$ .
- $\lambda$  is an arbitrary parameter.

In order to see how many equations can be set into an equation of the form (4.1), consider the second order differential equation

$$a_0(t)\ddot{y} + a_1(t)\dot{y} + (\lambda + a_2(t))y = 0. \quad (4.2)$$

which, considering  $a_0(t) > 0$ , can be rewritten as

$$\ddot{y} + \frac{a_1(t)}{a_0(t)}\dot{y} + \frac{\lambda + a_2(t)}{a_0(t)}y = 0. \quad (4.3)$$

Notice that the Sturm-Liouville equation (4.1) can be set as

$$\ddot{y} + \frac{\dot{p}(t)}{p(t)}\dot{y} + \frac{\lambda w(t) + q(t)}{p(t)}y = 0. \quad (4.4)$$

Comparing coefficients in (4.3) and (4.4) we obtain

$$\frac{\dot{p}(t)}{p(t)} = \frac{a_1(t)}{a_0(t)}$$

which by integration yields

$$p(t) = c \exp\left(\int^t \frac{a_1(\tau)}{a_0(\tau)} d\tau\right) \quad (4.5)$$

with  $c$  an arbitrary constant.

On the other hand, from

$$\frac{\lambda + a_2(t)}{a_0(t)} = \frac{\lambda w(t) + q(t)}{p(t)}$$

we obtain that

$$w(t) = \frac{p(t)}{a_0(t)} \quad (4.6)$$

$$q(t) = p(t) \frac{a_2(t)}{a_0(t)} \quad (4.7)$$

From the foregoing equation, (4.2) can be set into the Sturm-Liouville framework by only requiring  $a_i(t)$  to be such that  $p(t)$ ,  $r(t)$  and  $q(t)$  satisfy the restrictions given for (4.1). Notice that constant  $c$  in (4.5) can be set into any convenient value.

## 4.2 Sturm-Liouville BCs

Consider the set of homogeneous BCs

$$\mathcal{L}[y] = \begin{Bmatrix} \mathcal{L}_1[y] \\ \mathcal{L}_2[y] \end{Bmatrix} = \begin{Bmatrix} a_1y(a) + a_2\dot{y}(a) + b_1y(b) + b_2\dot{y}(b) \\ c_1y(a) + c_2\dot{y}(a) + d_1y(b) + d_2\dot{y}(b) \end{Bmatrix} = \begin{Bmatrix} 0 \\ 0 \end{Bmatrix} \quad (4.8)$$

**Definition 4.2.1.** Let  $f(t)$  and  $g(t)$  be two arbitrary functions that satisfy some given BCs such as (4.8), defined on  $[a, b]$ . If those functions also satisfy Green's formula:

$$\left[ p(t) \left( f^*(t) \frac{dg}{dt} - g(t) \frac{df^*}{dt} \right) \right]_{t=a}^b = 0, \quad (4.9)$$

where  $*$  denotes complex conjugation, then those homogeneous BCs are called the Sturm-Liouville BCs [18].

### 4.2.1 Twisted, periodic and anti-periodic BCs

Twisted BCs are defined as follows [15]:

$$\begin{aligned} y(a) &= \mu y(b) \\ \dot{y}(a) &= \mu \dot{y}(b) \\ p(a) &= p(b) \\ \mu &\in \mathbb{C}, |\mu| = 1 \end{aligned} \quad (4.10)$$

When  $\mu = 1$ , these conditions become the so called *periodic BCs*, and if  $\mu = -1$ , they are called *anti-periodic BCs*. Then twisted BCs can be regarded as a generalization of these two sets of BCs.

Let  $f, g$  be two functions that satisfy the twisted BCs, and let  $c_1, c_2 \in \mathbb{C}$  be two arbitrary constants. Then

$$\begin{aligned} c_1 f(a) + c_2 g(a) &= \mu [c_1 f(b) + c_2 g(b)] \\ c_1 \dot{f}(a) + c_2 \dot{g}(a) &= \mu [c_1 \dot{f}(b) + c_2 \dot{g}(b)] \end{aligned}$$

so, these BCs are homogeneous.

Now, replacing  $f$  and  $g$  in (4.9) we get

$$\begin{aligned} p(a) [f^*(a) \dot{g}(a) - g(a) \dot{f}^*(a)] - p(b) [f^*(b) \dot{g}(b) - g(b) \dot{f}^*(b)] &= \\ p(b) [f^*(a) \dot{g}(a) - g(a) \dot{f}^*(a) - f^*(b) \dot{g}(b) + g(b) \dot{f}^*(b)] &= \\ p(b) [\mu^* f^*(b) (\mu \dot{g}(b)) - \mu g(b) (\mu^* \dot{f}^*(b)) - f^*(b) \dot{g}(b) + g(b) \dot{f}^*(b)] &= 0 \end{aligned}$$

since  $p(a) = p(b)$  and  $\mu \mu^* = |\mu|^2 = 1$ . Then twisted BCs are Sturm-Liouville BCs.

### 4.3 Sturm-Liouville problem

Consider (4.1) and some Sturm-Liouville BCs. The Sturm-Liouville problem associated with these BCs is to find values for  $\lambda$  such that there exists a non-trivial solution  $\varphi$  of (4.1) which satisfies the Sturm-Liouville BCs. These values of  $\lambda$  correspond to the eigenvalues of a linear differential operator, and those non-trivial solutions are its associated eigenfunctions.

#### 4.3.1 Linear space of the Sturm-Liouville problem

Let  $L^2 = L^2[a, b, r(t)]$  be the space of quadratically integrable functions in  $[a, b]$  with weight function  $w(t)$ , defined over the complex numbers, i.e.  $f \in L^2$  if

$$\int_a^b w(t)|f(t)|^2 dt < \infty$$

The subspace  $L_{SL}^2 = L_{SL}^2[a, b, r(t)]$  of  $L^2$  is defined by restricting every function in  $L_{SL}^2$  to satisfy the homogeneous Sturm-Liouville BCs. The fact that these conditions are homogeneous is what allows  $L_{SL}^2$  to be a subspace of  $L^2$ . Using Dirac's notation [18], denote the elements  $\varphi$  of  $L_{SL}^2$  by  $|\varphi\rangle$ .

Define the inner product in  $L_{SL}^2$  as:

$$\langle f|g\rangle \triangleq \int_a^b w(t)f^*(t)g(t)dt, \quad (4.11)$$

and the induced norm:

$$\|f\| \triangleq \langle f|f\rangle^{\frac{1}{2}}, \quad (4.12)$$

#### 4.3.2 Sturm-Liouville operator

The Sturm-Liouville operator is defined as the linear differential operator:

$$\mathfrak{L} = \frac{1}{w(t)} \frac{d}{dt} \left( p(t) \frac{d}{dt} \right) + \frac{q(t)}{w(t)}, \quad (4.13)$$

where  $w(t)$ ,  $p(t)$  and  $q(t)$  satisfy the conditions given for the Sturm-Liouville equation (4.1).

In terms of the operator  $\mathfrak{L}$ , we can rewrite (4.1) as:

$$\mathfrak{L}y + \lambda y = 0. \quad (4.14)$$



Then the Sturm-Liouville problem is equivalent to finding the eigenvalues  $\lambda$  of the linear operator  $\mathfrak{L}$  and its associated eigenfunctions.

**Theorem 4.3.1.** [18]  $\mathfrak{L}$  is self-adjoint on the linear space  $L_{SL}^2$ , i.e. it satisfies:

$$\langle f, \mathfrak{L}g \rangle = \langle g, \mathfrak{L}f \rangle^*, \quad (4.15)$$

for all  $f, g \in L_{SL}^2$ .

*Proof.* Let  $f, g \in L_{SL}^2$ . By the definition of the scalar product:

$$\begin{aligned} \langle f, \mathfrak{L}g \rangle &= \int_a^b r(t) f^*(t) \mathfrak{L}g(t) dt \\ &= \int_a^b f^*(t) \frac{d}{dt} \left( p(t) \frac{d}{dt} g(t) \right) dt + \int_a^b f^*(t) q(t) g(t) dt \end{aligned}$$

where by integration by parts

$$\int_a^b f^*(t) \frac{d}{dt} \left( p(t) \frac{d}{dt} g(t) \right) dt = \left[ f^*(t) p(t) \frac{d}{dt} g(t) \right]_a^b - \int_a^b p(t) \frac{d}{dt} g(t) \frac{d}{dt} f^*(t) dt$$

Similarly we can find

$$\langle g, \mathfrak{L}f \rangle^* = \left[ g(t) p(t) \frac{d}{dt} f^*(t) \right]_a^b - \int_a^b p(t) \frac{d}{dt} f^*(t) \frac{d}{dt} g(t) dt + \int_a^b g(t) q(t) f^*(t) dt$$

which finally gives us Green's formula:

$$\langle f, \mathfrak{L}g \rangle - \langle g, \mathfrak{L}f \rangle^* = \left[ p(t) \left( f^*(t) \frac{dg}{dt} - g(t) \frac{df^*}{dt} \right) \right]_a^b = 0. \quad (4.16)$$

since, by definition, every function in  $L_{SL}^2$  satisfy the Sturm-Liouville BCs and so (4.16).  $\square$

The next theorem states some implication of the self-adjoint nature of the  $\mathfrak{L}$  operator

**Theorem 4.3.2.** [18] Let  $\mathfrak{L}$  be a self-adjoint linear differential operator. Then

- If  $\lambda \in \sigma(\mathfrak{L})$  then  $\lambda \in \mathbb{R}$ .
- Eigenfunctions associated with different eigenvalues are orthogonal.

*Proof.* Let  $\lambda_n$  and  $\lambda_m$  be two eigenvalues of  $\mathfrak{L}$  with respective associated eigenfunctions  $\varphi_n$  and  $\varphi_m$ . Then

$$\langle \varphi_n | \mathfrak{L} \varphi_m \rangle = \lambda_m \langle \varphi_n | \varphi_m \rangle$$

and similarly

$$\langle \varphi_m | \mathcal{L} | \varphi_n \rangle^* = \lambda_n^* \langle \varphi_m | \varphi_n \rangle^* = \lambda_n^* \langle \varphi_n | \varphi_m \rangle$$

By assumption  $\langle \varphi_n | \mathcal{L} | \varphi_m \rangle - \langle \varphi_m | \mathcal{L} | \varphi_n \rangle^* = 0$  so we get

$$(\lambda_m - \lambda_n^*) \langle \varphi_n | \varphi_m \rangle = 0 \quad (4.17)$$

Since eigenfunctions are, by definition, non-trivial, if  $m = n$  then  $\lambda_m = \lambda_m^*$  which implies  $\lambda_m \in \mathbb{R}$ . On the other hand, if  $m \neq n$ , then  $\langle \varphi_n | \varphi_m \rangle = 0$  which means  $\varphi_m$  and  $\varphi_n$  are orthogonal.  $\square$

### 4.3.3 Periodic and antiperiodic Sturm-Liouville problem

The periodic (respectively, anti-periodic) Sturm-Liouville problem is given by the Sturm-Liouville equation (4.1) plus the periodic (respectively, anti-periodic) Sturm-Liouville BCs, defined by (4.10) where  $\mu = 1$  (respectively,  $-1$ ).

**Theorem 4.3.3.** [19] *The eigenvalues of the periodic and antiperiodic Sturm-Liouville problem, respectively  $\lambda_i$  and  $\bar{\lambda}_i$ , are real and produce sequences such that:*

$$-\infty < \lambda_0 < \bar{\lambda}_1 \leq \bar{\lambda}_2 < \lambda_1 \leq \lambda_2 < \bar{\lambda}_3 \leq \bar{\lambda}_4 < \lambda_3 \leq \lambda_4 < \dots,$$

where the eigenvalue  $\lambda_0$  is never degenerate. If  $\lambda_{2m+1} < \lambda_{2m+2}$  (or  $\bar{\lambda}_{2m+1} < \bar{\lambda}_{2m+2}$ ) for some  $m \geq 0$ , then there exists an eigenfunction for each of these two eigenvalues. If  $\lambda_{2m+1} = \lambda_{2m+2}$  (or  $\bar{\lambda}_{2m+1} = \bar{\lambda}_{2m+2}$ ), then there are two linearly independent eigenfunctions for this degenerate eigenvalue.

*Proof.* Let  $\phi$  and  $\psi$  be the solutions of (4.1) which satisfy

$$\begin{aligned} \phi(0, \lambda) &= \psi(0, \lambda) = 1 \\ \dot{\phi}(0, \lambda) &= \dot{\psi}(0, \lambda) = 0 \end{aligned} \quad (4.18)$$

Choosing  $z = [y, py]$  as a state variable, the resulting linear system is linear Hamiltonian and its state transition matrix is symplectic, which means

$$p(t) [\phi(t, \lambda) \dot{\psi}(t, \lambda) - \dot{\phi}(t, \lambda) \psi(t, \lambda)] = 1 \quad (4.19)$$

For a solution satisfying the periodic BCs to exist, it is necessary and sufficient the existence of two constants  $c_1$  and  $c_2$  such that

$$\begin{aligned} c_1[\phi(b, \lambda) - 1] + c_2\psi(b, \lambda) &= 0 \\ c_1\dot{\phi}(b, \lambda) + c_2[\dot{\psi}(b, \lambda) - 1] &= 0 \end{aligned} \quad (4.20)$$

Rearranging (4.20) we get

$$\begin{bmatrix} (\phi(b, \lambda) - 1) & \psi(b, \lambda) \\ \dot{\phi}(b, \lambda) & (\dot{\psi}(b, \lambda) - 1) \end{bmatrix} \begin{bmatrix} c_1 \\ c_2 \end{bmatrix} = 0.$$

Then, a necessary and sufficient condition for (4.20) to have a non-trivial solution is that

$$\phi(b, \lambda)\dot{\psi}(b, \lambda) - \dot{\phi}(b, \lambda)\psi(b, \lambda) - \phi(b, \lambda) - \dot{\psi}(b, \lambda) + 1 = 0 \quad (4.21)$$

Without loss of generality, we can scale  $p(t)$  such that, at the boundaries,  $p(a) = p(b) = 1$ , by (4.19). Therefore condition (4.21) becomes

$$\text{fun}(\lambda) = \phi(b, \lambda) + \dot{\psi}(b, \lambda) = 2 \quad (4.22)$$

Similarly, the condition for a non-trivial solution of the anti-periodic Sturm-Liouville problem is

$$\text{fun}(\lambda) = \phi(b, \lambda) + \dot{\psi}(b, \lambda) = -2 \quad (4.23)$$

It should be clear to this point that the values of  $\lambda$  that satisfy (4.22) (respectively (4.23)) are the eigenvalues of the periodic (respectively anti-periodic) Sturm-Liouville problem.

By the Theorem of continuity with respect to parameters,  $\text{fun}(\lambda)$  is continuous, but it is also an entire function (Theorem 8.4 [19]).

The remain of the proof is a direct result of the following Lema.

**Lemma 4.3.1.** [19] Consider (4.1) with the BCs

$$y(a) = y(b) = 0$$

There exist a constant  $\vartheta_0$  such that the eigenvalues  $\mu_i$  of this problem can be arranged as

$$\vartheta_0 < \mu_0 < \mu_1 < \mu_2 < \dots$$

and

$$\text{fun}(\vartheta_0) \geq 2, \text{fun}(\mu_{2i}) \leq -2, \text{fun}(\mu_{2i+1}) \geq 2 \quad (4.24)$$

for  $i = 0, 1, \dots$

If  $\text{fun}(\lambda) = 2$  (respectively  $-2$ ) for some  $\lambda \neq \mu_i$ , then  $\lambda$  is a simple eigenvalue of the periodic Sturm-Liouville problem (respectively the anti-periodic Sturm-Liouville problem), and such  $\lambda$  also satisfies

$$\frac{d\text{fun}}{d\lambda} < 0 \text{ if } \lambda < \mu_0 \quad (4.25)$$

$$(-1)^i \frac{d\text{fun}}{d\lambda} > 0 \text{ if } \mu_i < \lambda < \mu_{i+1} \quad (4.26)$$

On the other hand, if  $\text{fun}(\mu_{2i+1}) = 2$  and  $d\text{fun}/d\lambda \neq 0$  at  $\lambda = \mu_{2i+1}$ , then  $\mu_{2i+1}$  is a simple eigenvalue of the periodic Sturm-Liouville problem. If  $\text{fun}(\mu_{2i+1}) = 2$  and  $d\text{fun}/d\lambda = 0$  at  $\lambda = \mu_{2i+1}$ , then  $\mu_{2i+1}$  has two linearly independent eigenfunctions, and, moreover

$$\frac{d^2\text{fun}}{d\lambda^2}(\mu_{2i+1}) < 0 \quad (4.27)$$

A similar argument holds for that case  $\text{fun}(\lambda) = -2$ . In this case, (4.27) changes sign.

□

Notice that equations (4.25), (4.26) and (4.27) ensure that the eigenvalues of the periodic and anti-periodic Sturm-Liouville problem to be pair-wise isolated between each other whenever  $i \neq 0$ .

#### 4.3.4 Twisted Sturm-Liouville problem

The twisted Sturm-Liouville problem is that formed by the Sturm-Liouville equation (4.1), and the twisted Sturm-Liouville BCs, defined by (4.10).

**Corollary 4.3.1.** [to Theorem 4.3.3] If we take  $\hat{\lambda}_i$ ,  $i = 1, 2, \dots$ , as the eigenvalues for the twisted BVP with  $\text{Im}(\mu) \neq 0$ , then these eigenvalues form a sequence that can be arranged with the eigenvalues of the periodic and anti-periodic Sturm-Liouville problem as:

$$-\infty < \lambda_0 < \hat{\lambda}_1 < \bar{\lambda}_1 \leq \bar{\lambda}_2 < \hat{\lambda}_2 < \lambda_1 \leq \lambda_2 < \hat{\lambda}_3 < \bar{\lambda}_3 \leq \bar{\lambda}_4 < \hat{\lambda}_4 < \lambda_3 \leq \lambda_4 < \dots \quad (4.28)$$

*Proof.* Following the same reasoning as in the previous theorem, the necessary and sufficient condition for the existence of a solution that satisfy the twisted BCs is:

$$\mu^2 - (\phi(b, \lambda) + \psi(b, \lambda))\mu + 1 = 0$$

which yields

$$\text{fun}(\lambda) = 2\text{Re}(\mu).$$

noticing  $|2\text{Re}(\mu)| < 2$  since  $\text{Im}(\mu) \neq 0$ .

From (4.25) and (4.26), function  $\text{fun}(\lambda)$  is monotonically increasing when  $|\text{fun}(\lambda)| < 2$ . This property and the continuity of  $\text{fun}(\lambda)$  ensures the fact that the eigenvalues  $\hat{\lambda}_i$  exist and are isolated points in  $\mathbb{R}$  producing a sequence that can be arranged as in (4.28).  $\square$



# Chapter 5

## The Sturm-Liouville problem and the Hill equation

Consider the Hill equation (1.3). This equation is in the form of the Sturm-Liouville equation by choosing  $p(t) = 1$ ,  $w(t) = 1$ ,  $q(t) = \beta f(t)$ ,  $\lambda = \alpha$ , and the Sturm-Liouville operator:

$$\mathfrak{L}_H = \frac{d^2}{dt^2} + \beta f(t) \quad (5.1)$$

Since, in this case,  $p(t)$  is constant, obviously  $p(0) = p(T)$ . Consequently, the conditions for the twisted Sturm-Liouville problem on  $[0, T]$  are fulfilled for a suitable choice of  $\mu$ . Moreover, since (1.3) is periodic with period  $T$ , then, by Theorem 2.1.4, and for a fixed value of  $\beta$ , the twisted Sturm-Liouville problem can be used in order to find those values of  $\alpha$  for which  $\mu$  is a Floquet multiplier of (1.3). The transition curves of the Hill equation can be computed by solving the periodic and the anti-periodic Sturm-Liouville problems, which are particular cases of the twisted Sturm-Liouville problem, in which  $\mu = 1$  and  $\mu = -1$ , respectively.

For an approximated solution of the twisted Sturm-Liouville problem, the next section shows an arbitrary order finite-difference scheme [8].

### 5.1 Finite difference scheme for the twisted Sturm-Liouville problem

Consider the uniform partition:

$$t_k = kh, \quad k \in \mathbb{Z}, \quad (5.2)$$

where

$$h = \frac{T}{N},$$

and  $N$  is a fixed natural number.

Take  $y \in L^2_{SL}$ , and define  $\eta_k = y(t_k)$ . Using a centered finite difference scheme [8], we can approximate  $\dot{y}(t_k)$  and  $\ddot{y}(t_k)$  respectively as

$$\dot{\eta}_k = \sum_{i=1}^n c_i (\eta_{k+i} - \eta_{k-i}) \quad (5.3)$$

and

$$\ddot{\eta}_k = d_0 \eta_k + \sum_{i=1}^n d_i (\eta_{k+i} + \eta_{k-i}) \quad (5.4)$$

where  $n$  defines the order of the error  $O(h^{2n})$ . Coefficients  $c_i$  and  $d_i$  are, respectively, the finite difference coefficients for the first and second derivative approximation.

For example, it can easily be seen that, for  $n = 1$ ,  $c_1 = 1/(2h)$ ,  $d_0 = -2/h^2$ , and  $d_1 = 1/h^2$ , result in

$$\begin{aligned} \dot{\eta}_k &= \frac{\eta_{k+1} - \eta_{k-1}}{2h} \\ \ddot{\eta}_k &= \frac{\eta_{k+1} - 2\eta_k + \eta_{k-1}}{h^2} \end{aligned}$$

Using (5.3) and (5.4), we can replace (4.14) by its approximation

$$r_k \mathcal{L}_h \eta_k + \Lambda r_k \eta_k = 0, \quad k = 0, 1, \dots, N \quad (5.5)$$

where  $\Lambda$  is an approximation of  $\lambda$ , and

$$\begin{aligned} r_k \mathcal{L}_h \eta_k &= p_k \dot{\eta}_k + \dot{p}_k \eta_k + q_k \eta_k \\ &= p_k \left( d_0 \eta_k + \sum_{i=1}^n d_i (\eta_{k+i} + \eta_{k-i}) \right) + \dot{p}_k \sum_{i=1}^n c_i (\eta_{k+i} - \eta_{k-i}) + q_k \eta_k \\ &= \sum_{i=1}^n (p_k d_i - \dot{p}_k c_i) \eta_{k-i} + (p_k d_0 + q_k) \eta_k + \sum_{i=1}^n (p_k d_i + \dot{p}_k c_i) \eta_{k+i} \\ &= \sum_{i=1}^n a(k, i) \eta_{k-i} + b(k) \eta_k + \sum_{i=1}^n c(k, i) \eta_{k+i} \end{aligned}$$



where

$$\begin{aligned} b(k) &= p_k d_0 + q_k \\ a(k, i) &= \begin{cases} p_k d_i - \dot{p}_k c_i, & \text{if } 1 \leq i \leq n \\ 0, & \text{otherwise} \end{cases} \\ c(k, i) &= \begin{cases} p_k d_i + \dot{p}_k c_i, & \text{if } 1 \leq i \leq n \\ 0, & \text{otherwise} \end{cases} \end{aligned}$$

Defining the discrete-time state variable  $\xi_k = (\eta_{k-n}, \eta_{k-n+1}, \dots, \eta_{k+n-1})^T \in \mathbb{R}^{2n}$  we can set (5.5) in the discrete-time state form

$$\xi_{k+1} = A_k \xi_k, \quad A_{k+N} = A_k. \quad (5.6)$$

The state transition matrix  $\Phi(k, k_0)$  of a discrete-time linear system is, in general, defined only for  $k \geq k_0$  as

$$\Phi(k, k_0) = \begin{cases} A_{k-1} A_{k-2} \dots A_{k_0} & \text{if } k > k_0 \\ I & \text{if } k = k_0 \end{cases}$$

where  $k_0$  defines the initial time. And, as  $A_k$  is periodic with period  $N$ , we have  $\Phi(k_0, k) = \Phi^{-1}(k, k_0)$ .

After the last discussion, it should be easy to see that the discrete-time version of the twisted BCs (4.10) in a finite difference framework, are

$$\eta_{j+N} = \mu \eta_j, \quad j = 0, 1, \dots, 2n-1 \quad (5.7)$$

noticing that, by uniqueness of solutions, these conditions are equivalent to

$$\eta_{j+N} = \mu \eta_j, \quad j = 0, 1, \dots, N-1$$

and, by  $\Phi(k+N, k_0+N) = \Phi(k, k_0)$ , this is also equivalent to

$$\eta_{k+N} = \mu \eta_k, \quad \forall k \in \mathbb{Z}.$$

Finally, introducing the  $N$ -dimensional vector

$$\eta = \begin{bmatrix} \eta_0 \\ \eta_1 \\ \vdots \\ \eta_{N-1} \end{bmatrix},$$

we can synthesize the finite-difference twisted Sturm-Liouville problem formed by (5.5) and (5.7) through the matrix equation

$$L\eta + \Lambda R\eta = 0 \quad (5.8)$$

where

$$L = \begin{bmatrix} b(0) & c(0,1) & c(0,2) & \dots & \mu^* a(0,3) & \mu^* a(0,2) & \mu^* a(0,1) \\ a(1,1) & b(1) & c(1,1) & \dots & \mu^* a(1,4) & \mu^* a(1,3) & \mu^* a(1,2) \\ a(2,2) & a(2,1) & b(2) & \dots & \mu^* a(2,5) & \mu^* a(2,4) & \mu^* a(2,3) \\ \vdots & \vdots & \vdots & \ddots & \vdots & \vdots & \vdots \\ \mu c(N-3,3) & \mu c(N-3,4) & \mu c(N-3,5) & \dots & b(N-3) & c(N-3,1) & c(N-3,2) \\ \mu c(N-2,2) & \mu c(N-2,3) & \mu c(N-2,4) & \dots & a(N-2,1) & b(N-2) & c(N-2,1) \\ \mu c(N-1,1) & \mu c(N-1,2) & \mu c(N-1,3) & \dots & a(N-1,2) & a(N-1,1) & b(N-1) \end{bmatrix} \quad (5.9)$$

noticing  $|\mu| = 1$ ,  $\implies 1/\mu = \mu^*$ , and

$$R = \begin{bmatrix} r_0 & 0 & \dots & 0 & 0 \\ 0 & r_1 & \dots & 0 & 0 \\ \vdots & \vdots & \ddots & \vdots & \vdots \\ 0 & 0 & \dots & r_{N-2} & 0 \\ 0 & 0 & \dots & 0 & r_{N-1} \end{bmatrix} = \text{diag}(r_i), \quad i = 0, 1, \dots, N-1. \quad (5.10)$$

Thus, with this framework, we are approximating the infinite-dimensional twisted Sturm-Liouville problem by the generalized eigenvalue-eigenfunction problem of matrices (5.9) and (5.10).

An algorithm to obtain the arbitrary order finite-difference coefficients is found in [20].

## 5.2 Stability chart

In Chapter 3, it was shown how Floquet multipliers of (1.3) are related with the stability of its trivial solution. Specifically, it was shown a conjugate pair of complex Floquet multipliers lying on the unit circle, mean, in general, bounded solutions; and, on the other hand, a real pair correspond, in general, to unbounded solutions (see Section 3.4). By these facts, Floquet multipliers  $\mu_{1,2} = 1$  and  $\mu_{1,2} = -1$  play an important role since they may or not correspond to bounded solutions, depending on the geometric multiplicity of  $\mu$ .

Consider (1.3). For a fixed value of  $\beta$ , values of  $\alpha$  for which Floquet multipliers are both 1 (respectively,  $-1$ ) can be found by solving the periodic (respectively, anti-periodic) Sturm-Liouville problem. By Theorem 4.3.3, these values of  $\alpha$  produce an increasing sequence of real numbers. By continuity with respect to parameters, if  $\beta$  is varied monotonically and continuously from  $\beta_0$  to  $\beta_n$ , where  $\beta_0 < \beta_n$ , and if the periodic Sturm-Liouville problem is solved for each  $\beta \in [\beta_0, \beta_n]$ , the result can be depicted as lines in the parameter space  $\alpha - \beta$ . These lines separate stable and unstable regions and are called *transition curves*. The graphical depiction of these boundaries is what is known as the Ince-Strutt diagram of the Hill equation.

To identify stable and unstable parameter regions, remember that stability can also be set as a function of the trace of the monodromy matrix,  $\text{tr}(M)$ , and noticing that, in this case,  $\text{fun}(\lambda) = \text{fun}(\alpha) = \text{tr}(M)$  (see Theorem 4.3.3). Notice  $|\text{tr}(M)| \geq 2$  whenever  $\alpha \in [\lambda_i, \lambda_{i+1}]$  or  $\alpha \in [\bar{\lambda}_i, \bar{\lambda}_{i+1}]$ , for  $i = 1, 2, \dots$ , where  $\{\lambda_i\}$  and  $\{\bar{\lambda}_i\}$  are, respectively, the eigenvalues of the periodic and anti-periodic Sturm-Liouville problems. Then this intervals define the instability intervals, i.e. regions of parameters for unbounded solutions.

As an example, consider (1.3) with  $f(t) = \cos(t)$ . This equation is known as *the Mathieu equation*. Its stability chart, obtained by the finite difference scheme for the twisted Sturm-Liouville problem using periodic and anti-periodic BCs, is shown in Figure 5.1. For its computation, values of  $\beta$  are taken from a uniform grid of finite number of values in the interval  $[0, 8]$ . As  $\cos(t + \pi) = -\cos(t)$ , and by the fact that the Hill equation, if stable, is uniformly stable, then the stability chart of the Mathieu equation is symmetric with respect to the  $\alpha$ -axis. White areas are stable parameter regions, i.e. regions of parameters for which solutions are bounded. Painted areas are unstable parameter regions. Borders for blue-painted areas (respectively, cyan-painted areas) were found by solving the periodic (respectively, anti-periodic) Sturm-Liouville problem.

Another important case of the Hill equation is the one with  $f(t) = \text{sign}(\cos(t))$ , which results in *the Meissner equation*. Its stability chart, obtained by the finite difference scheme, is shown in Figure 5.2. Again, it is symmetric with respect to the  $\alpha$ -axis. The interesting fact

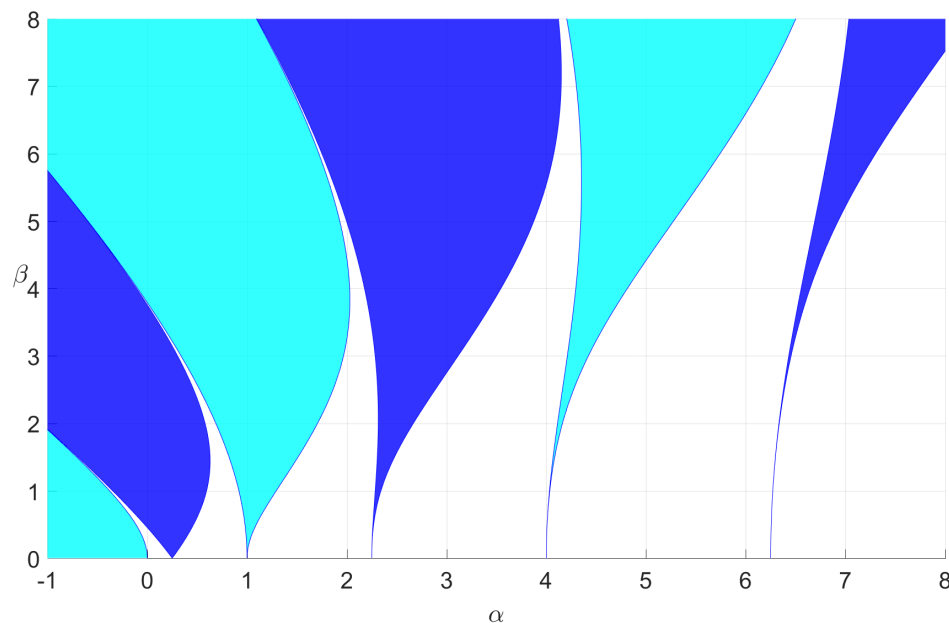


Figure 5.1: Stability chart of the Mathieu equation

about this particular equation is that its state transition matrix, and therefore its monodromy matrix, can be computed analytically since  $f(t)$  is piece-wise constant.

Finally, Figure 5.3 shows the stability chart of the Hill equation with

$$f(t) = \frac{d}{q} (\bar{f}(t) - m) \quad (5.11)$$

where

$$\bar{f}(t) = \frac{1}{(1.1 + \cos(t))},$$

$m$  is the mean value of  $\bar{f}(t)$ , and  $q$  and  $d$  are, respectively, the norm of  $(\bar{f}(t) - m)$  and the norm of  $\text{sign}(\cos(t))$  in  $L^2$ , the space of square integrable functions. The resultant function,  $f(t)$ , has zero mean value, and, moreover, has the same energy of  $\text{sign}(\cos(t))$ , i.e. the same  $L^2$  norm, which makes the stability chart of this equation suitable for comparison with the one corresponding to the Meissner equation. Notice that, in this case, there is no  $\theta$  such that  $f(t + \theta) = -f(t)$ , and its stability chart is not symmetric with respect to the  $\alpha$ -axis.

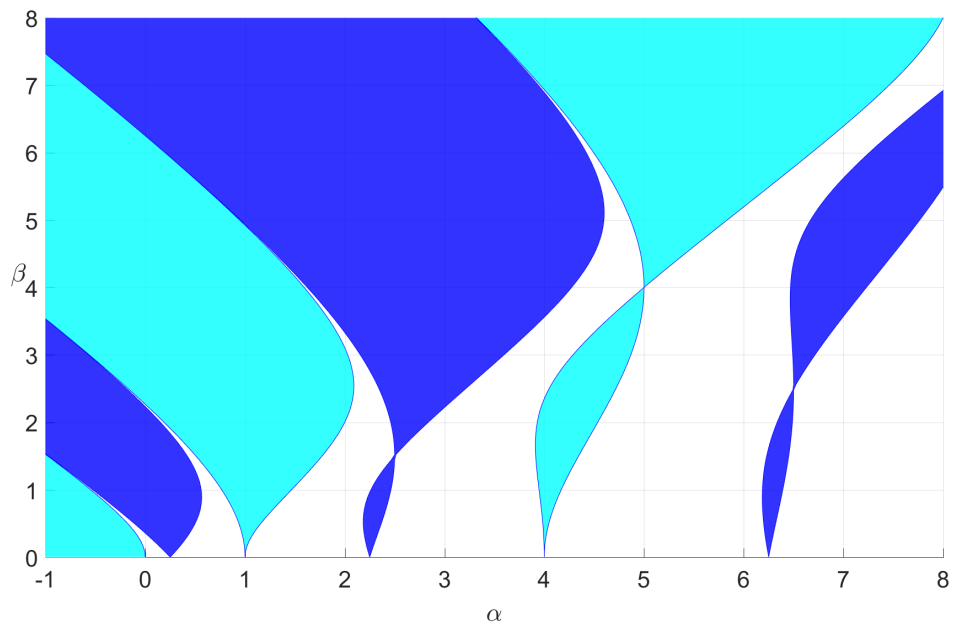
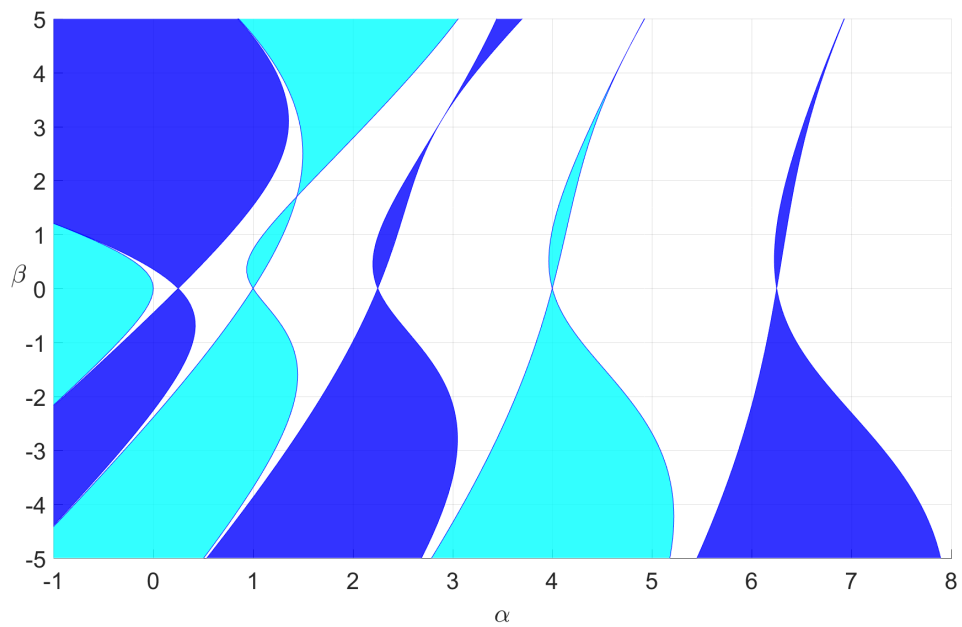


Figure 5.2: Stability chart of the Meissner equation

Figure 5.3: Stability chart of the Hill equation with  $f(t) = \frac{d}{q} \left( \frac{1}{(1.1 + \cos(t))} - m \right)$

### 5.3 Splitting lines

In [6], G. N. Jazar was able to compute those regions in the parameter space where  $k\pi$  periodic solutions exist using its energy-rate splitting chart algorithm on a  $\pi$ -periodic Mathieu equation. He called these curves *splitting lines*, arguing that these lines *split* each stable region. For this same reason, we shall borrow this name and use it to refer us to lines where periodic and aperiodic solutions exist inside stable zones of parameters.

Section 3.2 gives an explanation of Jazar's results. There is proven that at least one  $kT$ -periodic solution exist if and only if the Floquet multipliers of the Hill equation are  $k$ th unity-roots. And this, in fact, gives an extension of Jazar's results, since then: aperiodic solutions exist if and only if, the Floquet multipliers are not  $k$ th unity-roots for any  $k \in \mathbb{N}$ . For  $T = 2\pi$ , these this result can be rewritten as: at least one  $kT$ -periodic solution exist if and only if the imaginary part of a Floquet exponent of the Hill equation is a rational number.

One interesting phenomenon about  $kT$ -periodic solutions was pointed out by Rodriguez and Collado in [21]. They showed that, for the Hill equation with  $T = 2\pi$  and the splitting line associated with Floquet exponents:  $\rho_{1,2} = \pm i/k$ , all solutions of the non-homogeneous Hill equation, with parameters in the splitting line, become unbounded by the addition of a forcing input of the form:  $u(t) = \sum_{i=1}^n \cos(t/k_i)$ , where there is at least one  $1 \leq j \leq n$  such that  $k_j = k$ . Moreover, they showed that this phenomenon can arise in several splitting lines at the same time by the same input, provided there is a  $k_i$  associated with each line. Contrary to the stability chart, these unstable lines of parameters vanish with the addition of damping, although, as in the harmonic oscillator case, near those parameters, solutions may still show high amplitude oscillations. Rodriguez and Collado named the unstable splitting lines as *resonance lines*.

#### 5.3.1 Splitting lines of periodic solutions

Consider again the Mathieu equation. Figure 5.4 shows a pair of lines inside each stable zone corresponding to a parameter configuration for  $10\pi$ -periodic solutions. For parameters inside the solid lines, Floquet multipliers are  $\mu_{1,2} = e^{\pm j2\pi/5}$ , whereas for the dashed lines  $\mu_{1,2} = e^{\pm j2\pi(2/5)}$ . Since, for both cases, Floquet multipliers are primitive *5th* unity-roots, solutions at these parameter configurations are  $5T = 10\pi$  periodic. Figure 5.5 shows a numerical solution corresponding a point inside a dashed line. Red dashed lines are drawn at  $t = 10\pi$  and  $t = 20\pi$  to highlight its periodicity.

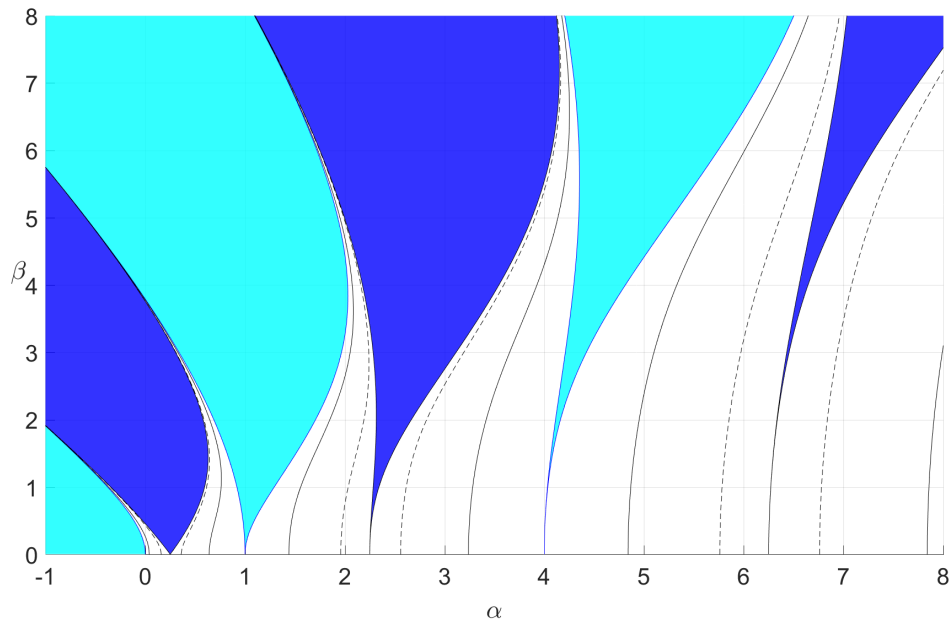


Figure 5.4: Stability chart of the Mathieu equation with splitting lines correspondent to  $10\pi$ -periodic solutions.

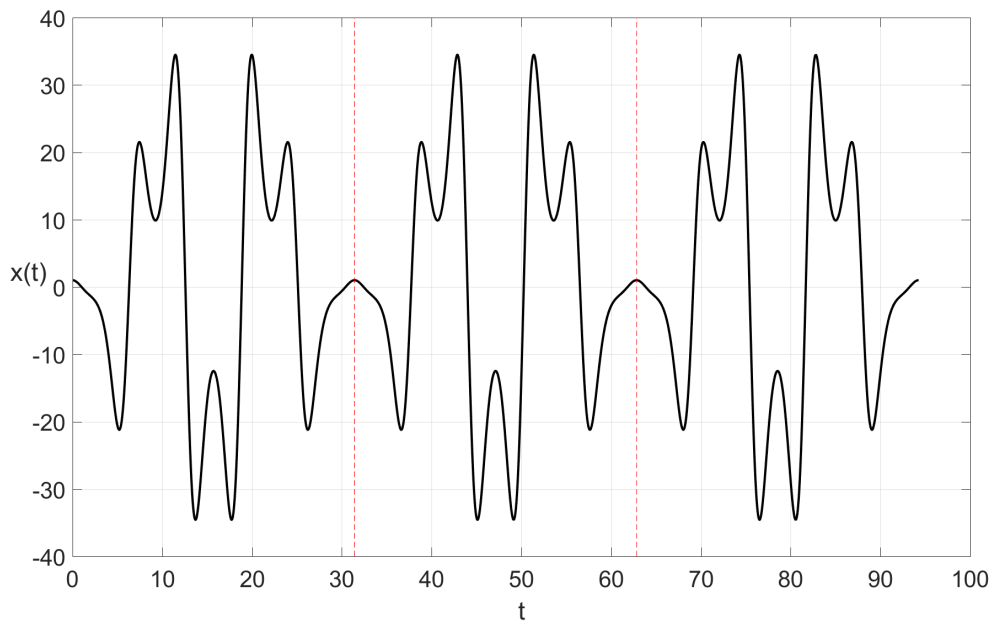


Figure 5.5:  $10\pi$ -periodic solution of the Mathieu equation for initial condition  $x(0) = [1, 0]^T$  and computed parameters  $\alpha = 2.821159061221791$  and  $\beta = 2$  for Floquet multipliers  $\mu_{1,2} = e^{\pm j2\pi(2/5)}$ .

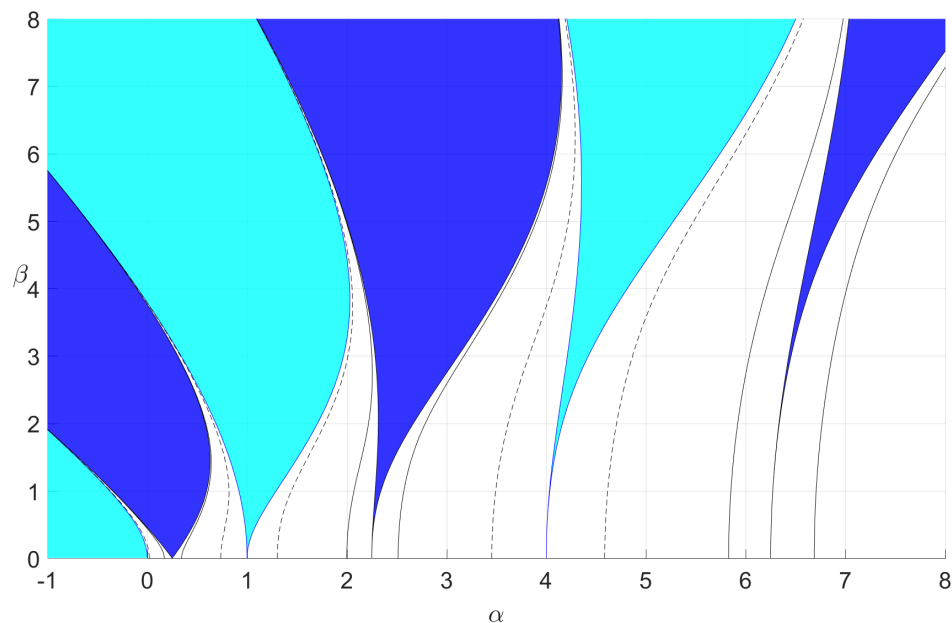


Figure 5.6: Stability chart of the Mathieu equation with splitting lines correspondent to aperiodic solutions.

### 5.3.2 Splitting lines of aperiodic bounded solutions

Figure 5.6 shows the stability chart of the Mathieu equation with a pair of lines inside each stable region. Dashed lines correspond to Floquet multipliers  $\mu_{1,2} = e^{\pm j2\pi^2}$  and solid lines with  $\mu_{1,2} = e^{\pm j2\pi\sqrt{2}}$ . This means the imaginary part of Floquet exponents are irrational numbers and, therefore, they correspond to aperiodic solutions. Figure 5.7 shows a numerical solution correspondent to a point inside a dashed line. This solution seem to repeat itself at  $t = 14\pi$ , which is consistent with the fact that a rational approximation of  $\pi$  is  $22/7$ . Nevertheless, a careful look at the trajectory inside the blue circles shows this solution is not periodic with period  $14\pi$ .

### 5.3.3 Linear resonance

The reason behind the phenomenon of resonance or unstable splitting lines, is due to the fact that Hill's equation, at a stable parameter configuration, is Lyapunov equivalent to an infinite set of harmonic oscillators (as it was shown in Section 3.4). In fact, we shall show examples of how linear resonance may occur even at splitting lines correspondent to aperiodic solutions, and the number of resonant frequencies for this lines is non unique.



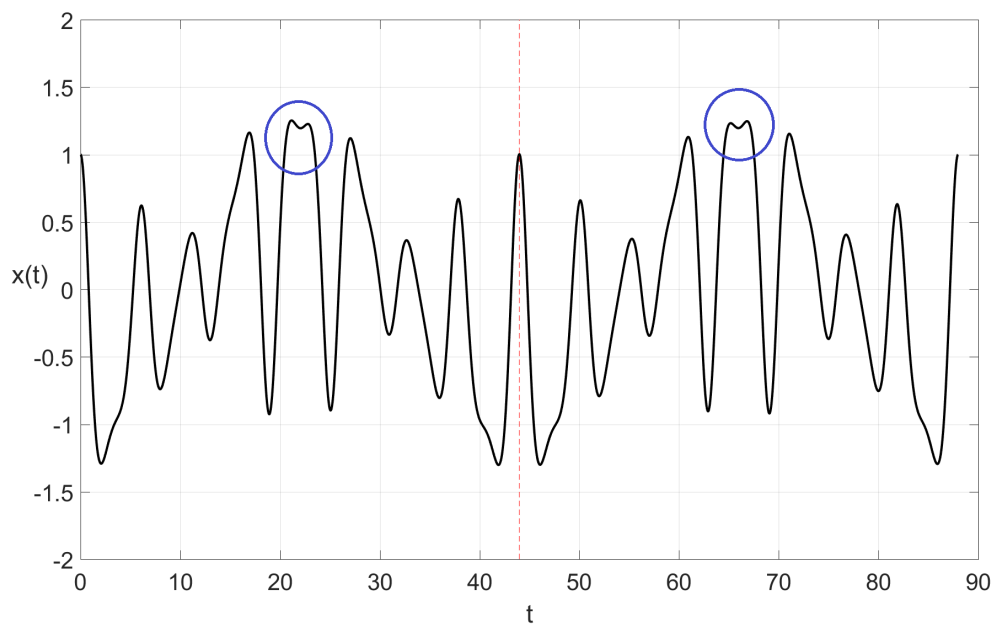


Figure 5.7: Aperiodic solution of the Mathieu equation for initial condition  $x(t) = [1, 0]^T$  and computed parameters  $\alpha = 1.781357855842370$  and  $\beta = 2$  for Floquet multipliers  $\mu_{1,2} = e^{\pm j2\pi^2}$ .

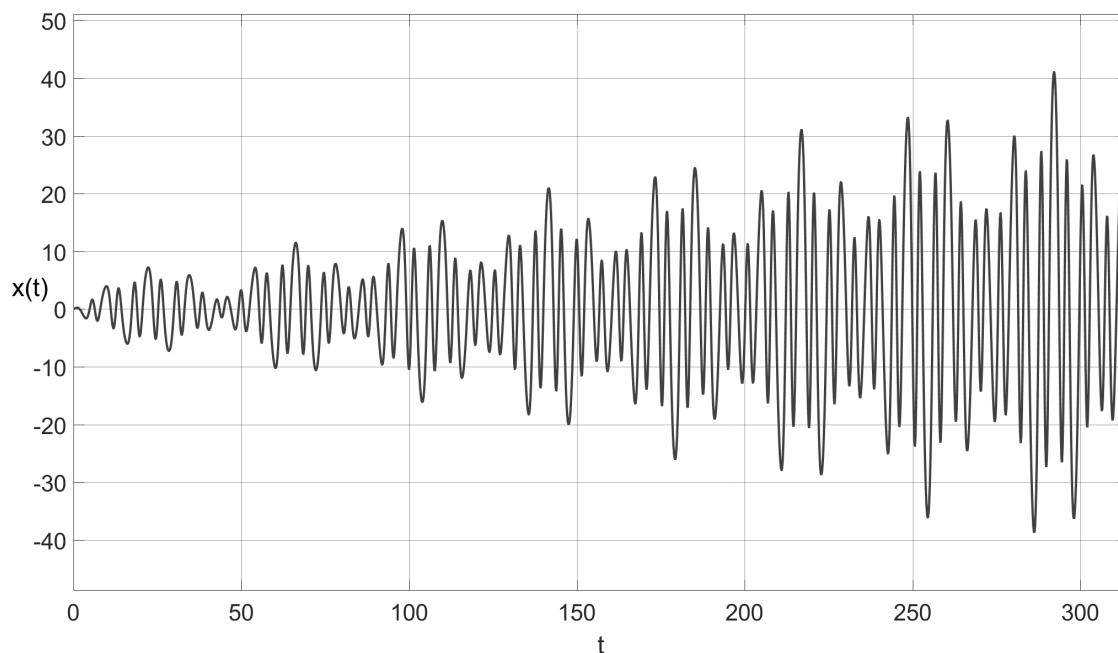


Figure 5.8: Resonant aperiodic solution of Mathieu's equation with forcing input  $u(t) = \cos(\sqrt{2}t)$ , initial condition  $x(t) = [0.05, 0]^T$ , and computed parameters  $\alpha = 2.787354403706198$  and  $\beta = 2$  for Floquet multipliers  $\mu_{1,2} = e^{\pm j2\pi\sqrt{2}}$ .

Figures 5.8 and 5.8 show, respectively, numerical solutions of the non-homogeneous Mathieu's equation with forcing inputs  $u(t) = \cos(\sqrt{2}t)$  and  $u(t) = \cos((\sqrt{2} + 1)t)$ . Values of  $\alpha$  and  $\beta$  for this solutions correspond to a point inside a solid line in Figure 5.6, i.e., to a line of aperiodic solutions. These solutions imply that linear resonance may occur at aperiodic splitting lines and also that they may be unstabilized by more than one resonance frequency.

## 5.4 Addition of damping

Consider the damped Hill equation:

$$\ddot{y} + \delta\dot{y} + (\alpha + \beta f(t))y = 0.$$

with  $\delta > 0$ . By (4.5), (4.6) and (4.7), this equation can be set on a Sturm-Liouville form choosing  $p(t) = e^{\delta t}$ ,  $w(t) = e^{\delta t}$ ,  $q(t) = \beta f(t)e^{\delta t}$ ,  $\lambda = \alpha$ . Since  $p(0) \neq p(T)$ , the Sturm-

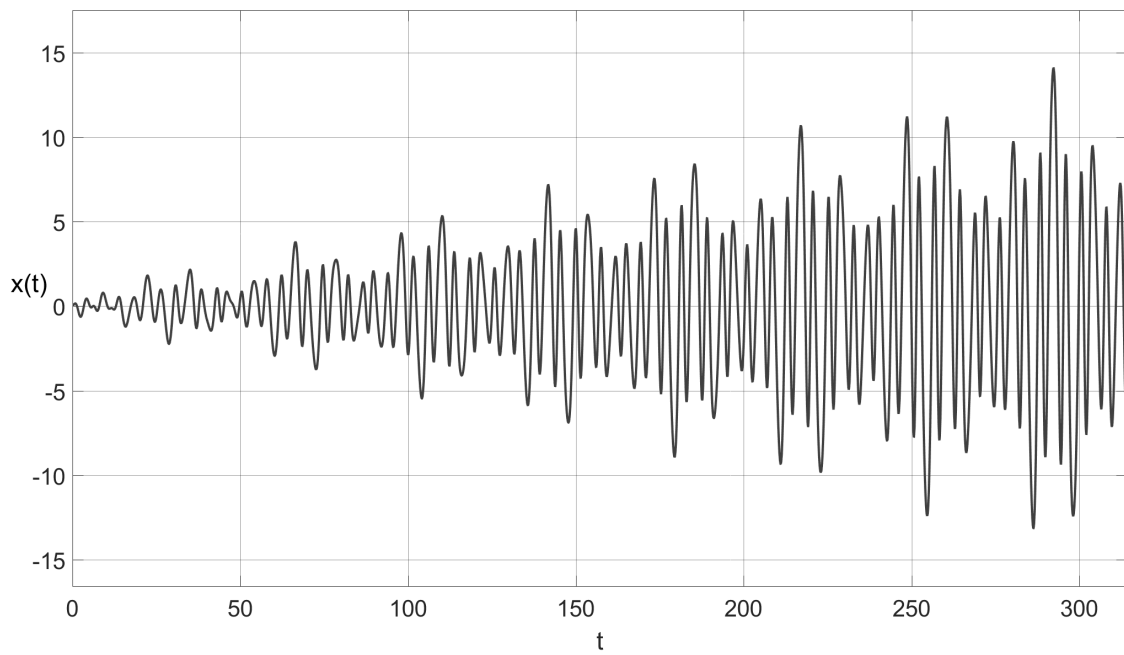


Figure 5.9: Resonant aperiodic solution of Mathieu's equation with forcing input  $u(t) = \cos((\sqrt{2} + 1)t)$ , initial condition  $x(t) = [0.05, 0]^T$ , and computed parameters  $\alpha = 2.787354403706198$  and  $\beta = 2$  for Floquet multipliers  $\mu_{1,2} = e^{\pm j2\pi\sqrt{2}}$ .

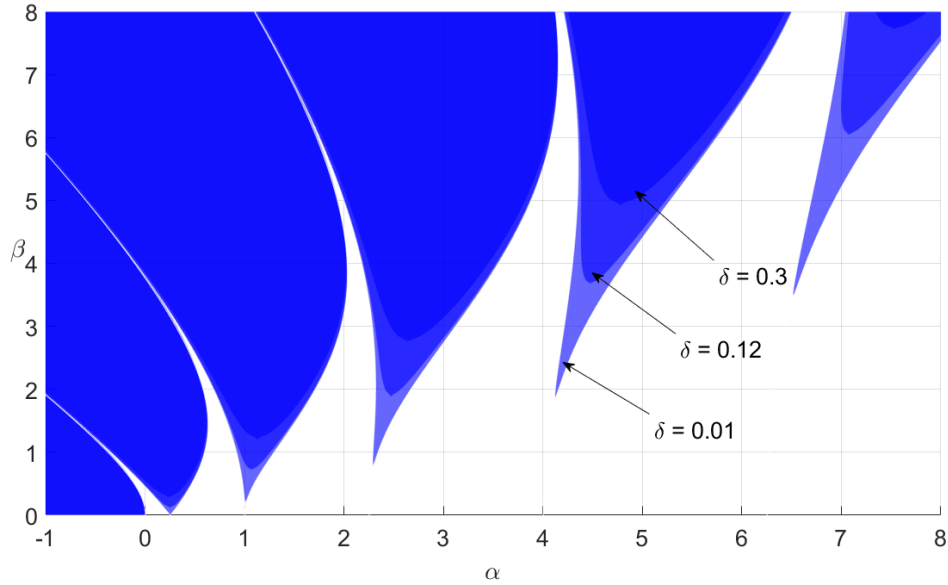


Figure 5.10: Stability charts of damped Mathieu's equation for three different damping coefficient values

Liouville operator

$$\frac{d}{dt} \left( e^{\delta t} \frac{d}{dt} \right) + \beta f(t) e^{\delta t}$$

is not self-adjoint in  $L_{SL}^2$ . This implies that the values of  $\alpha$  that solve the twisted Sturm-Liouville problem for this equation will not form a sequence of real numbers. Instead, only a finite number of values will be real.

The stability chart of this equation can be obtained as the generalized eigenvalue problem of matrices (5.9) and (5.10).

Figure 5.10 shows the stability chart of the damped Mathieu equation for three different values of the damping coefficient  $\delta$ . It can be noticed that Arnold tongues appear to lift from the  $\alpha$ -axis.

## 5.5 Lamé equation

The Lamé equation is defined as

$$\ddot{y} + (\bar{\alpha} - \beta(\beta + 1)\gamma \text{sn}^2(t)) y = 0 \quad (5.12)$$

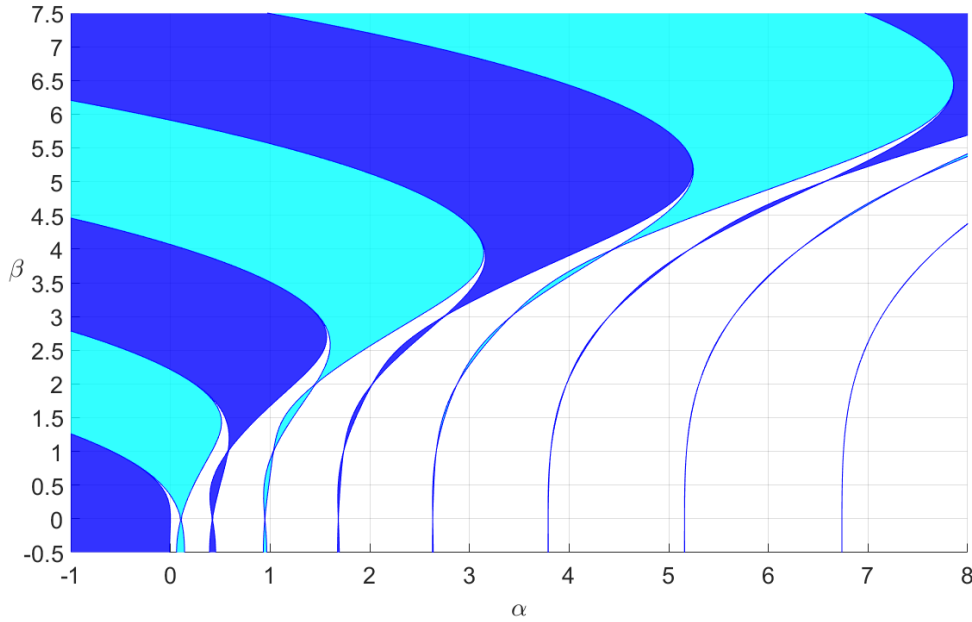


Figure 5.11: Ince-Strutt diagram of the Lamé equation

where  $\text{sn}(t)$  is a Jacobi elliptic function with  $\gamma$  as its modulus. For  $t \in \mathbb{R}$ , the period of  $\text{sn}^2(t)$  is  $2K$ , where  $K$  is given by

$$K = \int_0^{\pi/2} \frac{d\tau}{\sqrt{1 - \gamma \sin^2(\tau)}}.$$

Obviously,  $\text{sn}^2(t)$ , as it is non-trivial, has a non zero mean value  $m$ . Then, it can be set as  $\text{sn}^2(t) = h(t) + m$ , where  $h(t)$  is a  $2K$ -periodic function of zero mean value. Setting  $\alpha = \bar{\alpha} - \beta(\beta + 1)\gamma m$ , we can rewrite (5.12) as

$$\ddot{y} + (\alpha - \beta(\beta + 1)\gamma h(t))y = 0. \quad (5.13)$$

Figure 5.11 shows the stability chart of Lamé's equation (5.13), with  $\gamma = 0.999$ . As stated in Theorem 3.5.1, coexistence points arise at integer values of  $\beta$ , and, moreover, the number of instability intervals at these values is finite.

Notice that  $\beta = 0$  and  $\beta = -1$  make the time-varying term vanish, so the Ince-Strutt diagram is not symmetric with respect to the  $\alpha$ -axis. Nevertheless, for  $b \in \mathbb{R}$ , both  $\beta = b$  and  $\beta = -b - 1$  satisfy  $\beta(\beta + 1) = b(b + 1)$ , then the Ince-Strutt diagram is symmetric with respect to an horizontal axis drawn at  $\beta = -0.5$ .

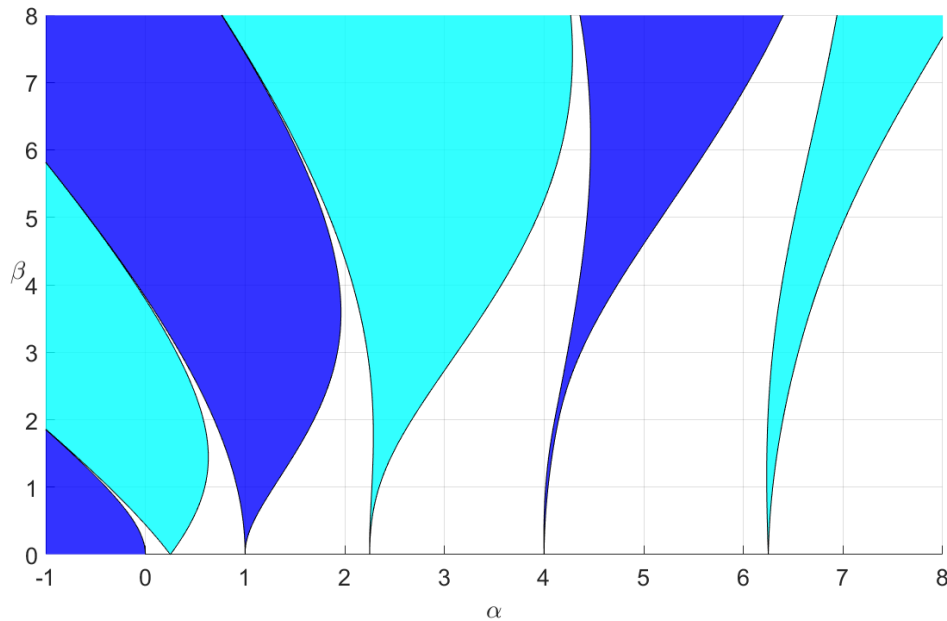


Figure 5.12: Diagram obtained by solving the periodic and the anti-periodic Sturm-Liouville problems for the quasi-periodic Hill equation (5.14), for  $f(t) = \cos(t) + 0.2 \sin(2\pi t)$ .

## 5.6 Quasi-periodic Hill equation

Consider

$$\ddot{y} + (\alpha + \beta f(t))y = 0 \quad (5.14)$$

where  $f(t) = f(\omega_1 t, \omega_2 t)$ , where  $\omega_1$  and  $\omega_2$  are rationally independent, i.e. there is no rational number  $q \in \mathbb{Q}$  such that  $\omega_1 = q\omega_2$ . This implies  $f(t)$  is not periodic of any period.

Since (5.14) is not a periodic linear differential equation, then Floquet theory does not apply and we can not get information about stability from it. Nevertheless, since the twisted Sturm-Liouville problem does not require the periodicity property of the  $q(t)$  coefficient in the Sturm-Liouville equation, we can still obtain a sequence of real values of  $\alpha$ , for a fixed  $\beta$ , such that a solution of (5.14) satisfies the twisted BCs.

In particular, choosing  $f(t) = \cos(t) + 0.2 \sin(2\pi t)$ , we can obtain the diagram shown in Figure 5.12 by solving the periodic and the anti-periodic Sturm-Liouville problems for (5.14), for the cyan-colored areas and the blue-colored areas, respectively. However, this diagram has no stability interpretation as in the case of the Ince-Strutt diagram of the Hill equation, nor its borders can be related with periodic solutions of period  $T$  and  $2T$ .

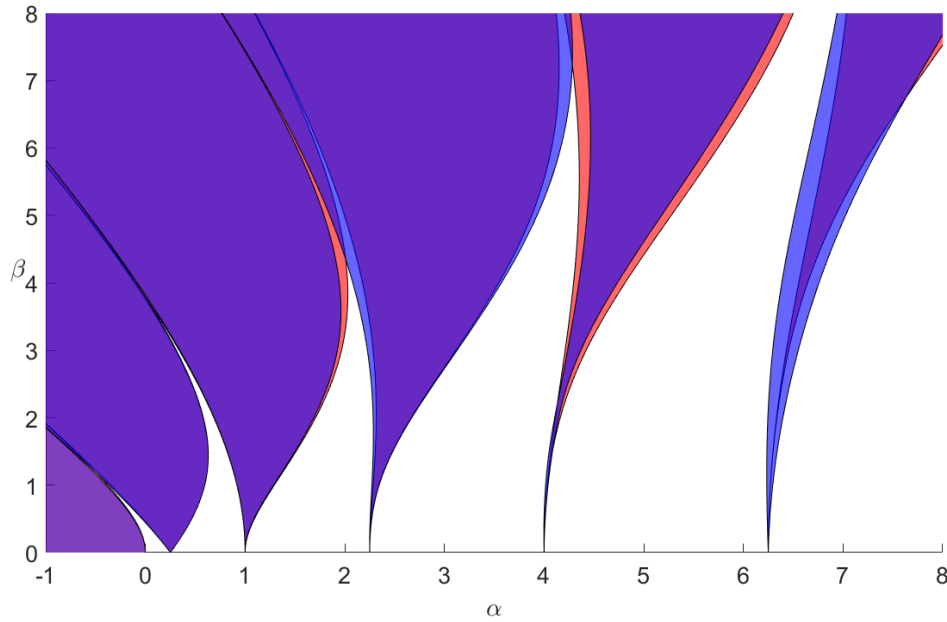


Figure 5.13: Superimposition of the diagrams in Figures 5.12 and 5.1.

Figure 5.13 shows the superimposed diagrams of 5.12, in blue, at the front-ground, and 5.1, in red, at the back-ground, where the intersection of these two diagrams is shown in purple.

## 5.7 Comparative study

In order to compare the accuracy of the finite-difference approach with the results obtained by Jazar [6] and the spectral methods [7], consider the Mathieu equation:

$$\ddot{y} + (\alpha + 2\beta \cos(2t))y = 0. \quad (5.15)$$

Tables 5.1 and 5.2 show, respectively, the first five values of  $\alpha$  for the Ince-Strutt diagram of the Mathieu equation obtained by the spectral method, using  $N = 50$ , and Jazar's algorithm. Tables 5.3 and 5.4, on the other hand, show some computed values of the Ince-Strutt diagram of the Mathieu equation using the finite-difference approach, with, respectively,  $n = 2$  and  $n = 4$ , and both  $N = 300$ . Figures 5.14 and 5.15 show, respectively, the Ince-Strutt diagrams correspondent to Tables 5.1 and 5.3. No difference can be appreciated between the two charts.

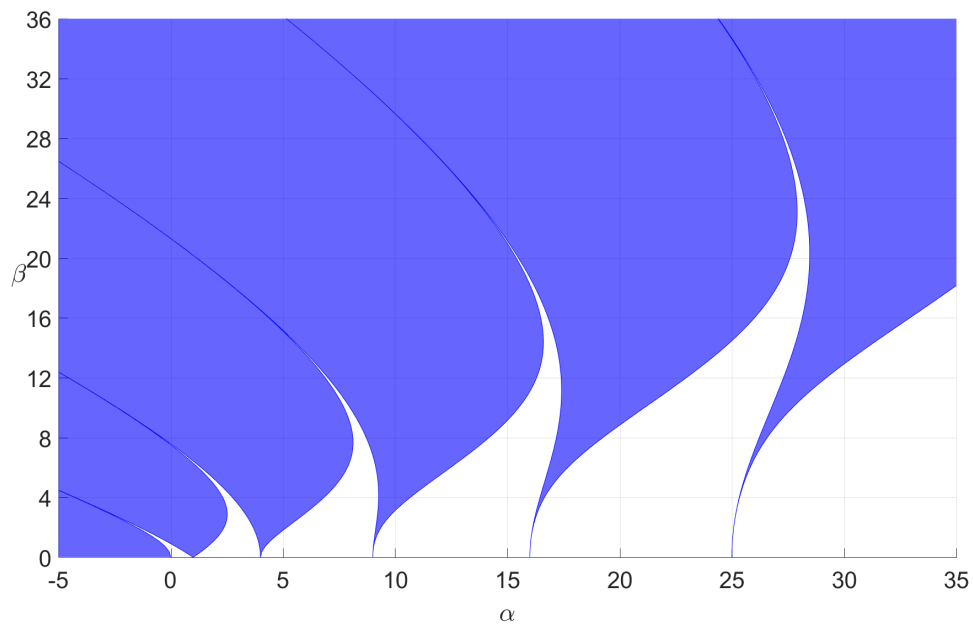


Figure 5.14: Ince-Strutt diagram of the Mathieu equation correspondent to Table 5.1

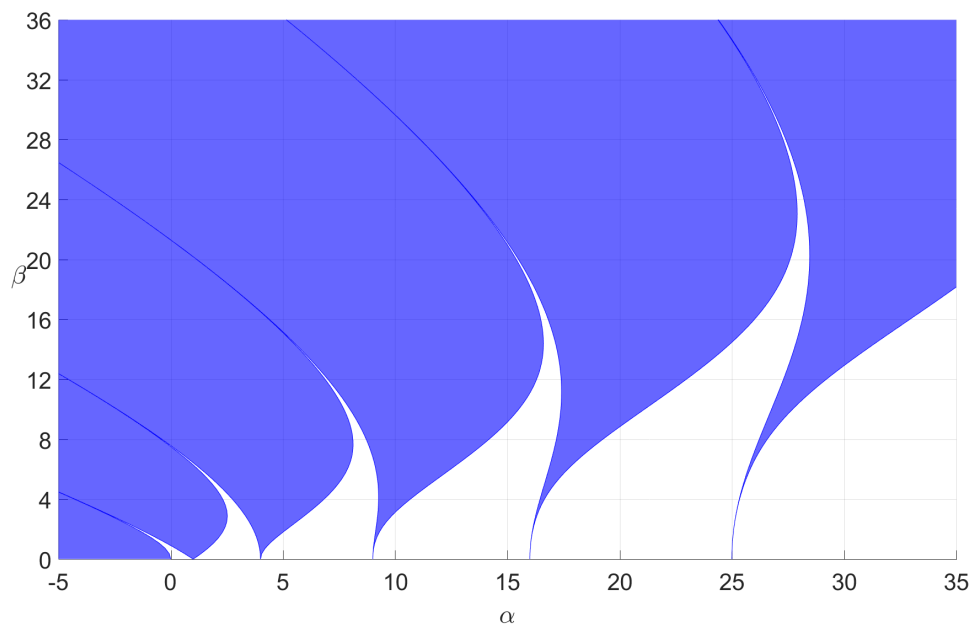


Figure 5.15: Ince-Strutt diagram of the Mathieu equation correspondent to Table 5.3



Table 5.1: Some values of the Ince-Strutt diagram obtained using the spectral method algorithm

$\beta$	$\alpha_0$	$\alpha_1$	$\alpha_2$	$\alpha_3$	$\alpha_4$
0	0	1	1	4	4
1	-0.455138604	-0.110248816	1.859108072	3.917024772	4.371300982
3	-2.834391889	-2.785379699	2.519039087	3.276921969	6.045196852
5	-5.800046020	-5.790080598	1.858187541	2.099460445	7.449109739
8	-10.606729235	-10.605368138	-0.435943601	-0.389361770	8.115238830
14	-20.776055312	-20.776000421	-6.893400533	-6.890700676	5.736312349
20	-31.313390070	-31.313386166	-14.491301425	-14.491063255	1.154282885
28	-45.673369639	-45.673369448	-25.561747094	-25.561732907	-6.588062973
32	-52.942222963	-52.942222914	-31.365154447	-31.365150511	-10.914353386
36	-60.255567891	-60.255567877	-37.302639122	-37.302637954	-15.466770336

Table 5.2: Some values of the Ince-Strutt diagram of the Mathieu equation obtained by Jazar

$\beta$	$\alpha_0$	$\alpha_1$	$\alpha_2$	$\alpha_3$	$\alpha_4$
0	0	1	1	4	4
1	-0.455138604	-0.110249001	1.8591084	3.9170245	4.3713010
3	-2.834391889	-2.7853799	2.5190390	3.2769217	6.0451972
5	-5.800046020	-5.7900808	1.858187541	2.0994601	7.4491094
8	-10.606729235	-10.6053683	-0.435943601	-0.3893621	8.11523883
14	-20.776055312	-20.7760006	-6.893400533	-6.890701	5.736312349
20	-31.313390070	-31.3133864	-14.491301425	-14.4910636	1.154228590
28	-45.673369663	-45.673369545	-25.561747709	-25.5617332	-6.588062973
32	-52.942222964	-52.942222939	-31.365154448	-31.3651508	-10.914353387
36	-60.255567891	-60.2555681	-37.302639123	-37.3026383	-15.466770337

Table 5.3: Some values of the Ince-Strutt diagram of the Mathieu equation obtained using the finite-difference scheme with  $N = 300$  and  $n = 2$ 

$\beta$	$\alpha_0$	$\alpha_1$	$\alpha_2$	$\alpha_3$	$\alpha_4$
0	0	1	1	4	4
1	-0.4551386050	-0.1102488183	1.8591080704	3.9170247607	4.3713009713
3	-2.834391897	-2.785379707	2.519039060	3.276921928	6.045196809
5	-5.800046038	-5.790080616	1.858187458	2.099460351	7.449109598
8	-10.60672927	-10.60536817	-0.435943806	-0.3893619812	8.115238355
14	-20.77605540	-20.77600051	-6.893401075	-6.890701220	5.736310792
20	-31.31339023	-31.31338632	-14.49130240	-14.49106423	1.154279908
28	-45.67336990	-45.67336971	-25.56174878	-25.56173459	-6.588068291
32	-52.94222329	-52.94222324	-31.36515654	-31.36515260	-10.91436005
36	-60.25556828	-60.25556827	-37.30264165	-37.30264048	-15.46677844

Table 5.4: Some values of the Ince-Strutt diagram obtained using the finite-difference scheme with  $N = 300$  and  $n = 5$ 

$\beta$	$\alpha_0$	$\alpha_1$	$\alpha_2$	$\alpha_3$	$\alpha_4$
0	0	1	1	4	4
1	-0.4551386041	-0.1102488170	1.859108072	3.917024772	4.371300982
3	-2.834391889	-2.785379699	2.519039087	3.276921969	6.045196852
5	-5.800046020	-5.790080598	1.858187541	2.099460445	7.449109739
8	-10.60672923	-10.60536813	-0.4359436013	-0.3893617702	8.115238830
14	-20.77605531	-20.77600042	-6.893400533	-6.890700676	5.736312349
20	-31.313390070	-31.313386166	-14.491301425	-14.491063255	1.1542828852
28	-45.673369639	-45.673369448	-25.561747094	-25.561732907	-6.5880629730
32	-52.942222963	-52.942222914	-31.365154447	-31.365150511	-10.914353386
36	-60.255567891	-60.255567877	-37.302639122	-37.302637954	-15.466770336

# Chapter 6

## A mechanical system with periodically varying moment of inertia

This chapter shows an example of a mechanical system with periodically time-varying moment of inertia [22], as the one shown in Figure 6.1. This system is modeled by a linear periodic second order ordinary differential equation, which can be seen as an equation of the Sturm-Liouville type. A bifurcation diagram, highlighting the stable and unstable parameter values in the parameter space  $\alpha - \beta$ , will be computed using the finite difference method described in Chapter 5.

### 6.1 Linear model

Consider the system shown in Figure 6.1. It consists on a massless elastic shaft, with stiffness  $c$ , driving a rigid disk, with moment of inertia  $J_0$ , in which, at the same time, there are two masses  $m$ , symmetrically placed, and moving along its radius according to the motion law:

$$r(\omega\tau, \beta) = r_0 + \beta f(\omega\tau).$$

where  $r_0$  is the nominal distance of the masses from the vertical axis of the shaft. Here,  $\beta$  and  $\omega$  are, respectively, the excitation amplitude and frequency, and  $f(\tau)$  is a twice continuously differentiable periodic function of period  $2\pi$  with zero mean value.

The total moment of inertia of the system is

$$J(\omega\tau, \beta) = J_0 + 2m(r_0 + \beta f(\omega\tau))^2. \quad (6.1)$$

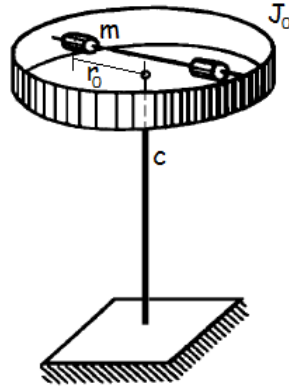


Figure 6.1: Elastic shaft with a rigid disk with two radially moving masses. (image borrowed from [22])

If  $J_0$  is large enough, we can neglect the dissipation term, and the equation of motion is then:

$$\frac{d}{d\tau}(J(\omega\tau, \beta) \frac{d}{d\tau}\theta) + c\theta = 0 \quad (6.2)$$

where  $\theta$  is the twisting angle of the disc with respect to the shaft axis.

## 6.2 Bifurcation diagram

Define  $t = \omega\tau$ , so

$$\frac{d}{d\tau} = \omega \frac{d}{dt}.$$

Then (6.2) boils down into

$$\omega^2 \frac{d}{dt} \left( J(t, \beta) \frac{d}{dt} \theta \right) + c\theta = 0.$$

Define

$$\alpha = \frac{c}{b\omega^2},$$

where

$$b = (J_0 + 2mr_0^2),$$

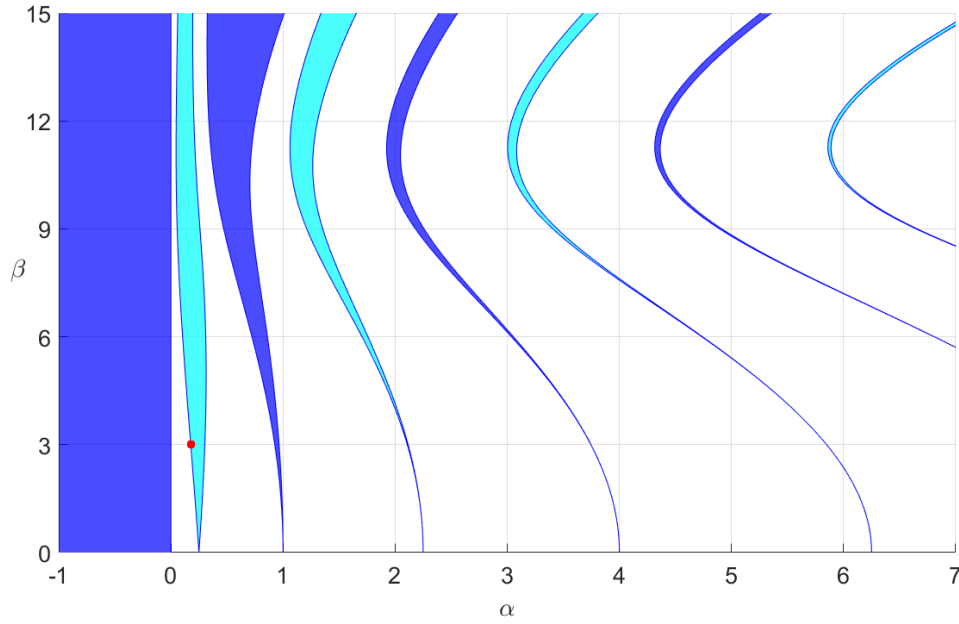


Figure 6.2: Bifurcation diagram for the elastic shaft system.

to obtain

$$\frac{d}{dt} \left( \frac{J(t, \beta)}{b} \frac{d}{dt} \theta \right) + \alpha \theta = 0. \quad (6.3)$$

Set  $f(t) = \cos(t)$ ,  $m = 10$ ,  $r_0 = 10$ ,  $J_0 = 100$ . Figure 6.2 shows the bifurcation diagram depicting the stable (white) and unstable (painted) parameter regions for (6.3). The borders of the cyan-painted areas correspond to parameters where a  $2\pi$ -periodic solution exist, and the borders of the blue-painted areas correspond to parameters where a  $4\pi$ -periodic solution exist. The diagram was computed using the finite-difference solution method for the periodic and anti-periodic Sturm-Liouville problems, for the blue-painted areas and cyan painted areas, respectively, choosing:  $\lambda = \alpha$ ,  $w(t) = 1$ ,  $q(t) = 0$ , and  $p(t) = p(t, \beta) = J(t, \beta)/b$ .

The point  $p_0 = (0.176867620295921, 3)$ , highlighted with a red dot in Figure 6.2, lies at a transition curve where a periodic solution of period  $4\pi$  exists. Figures 6.3 and 6.4 show, respectively, numerical solutions for points  $p_1 = (0.1775, 3)$  and  $p_2 = (0.175, 3)$  for initial condition  $x(t) = [1, 0]^T$ . As expected, solution for point  $p_1$  is unbounded and grows exponentially, while for point  $p_2$  it remains bounded.

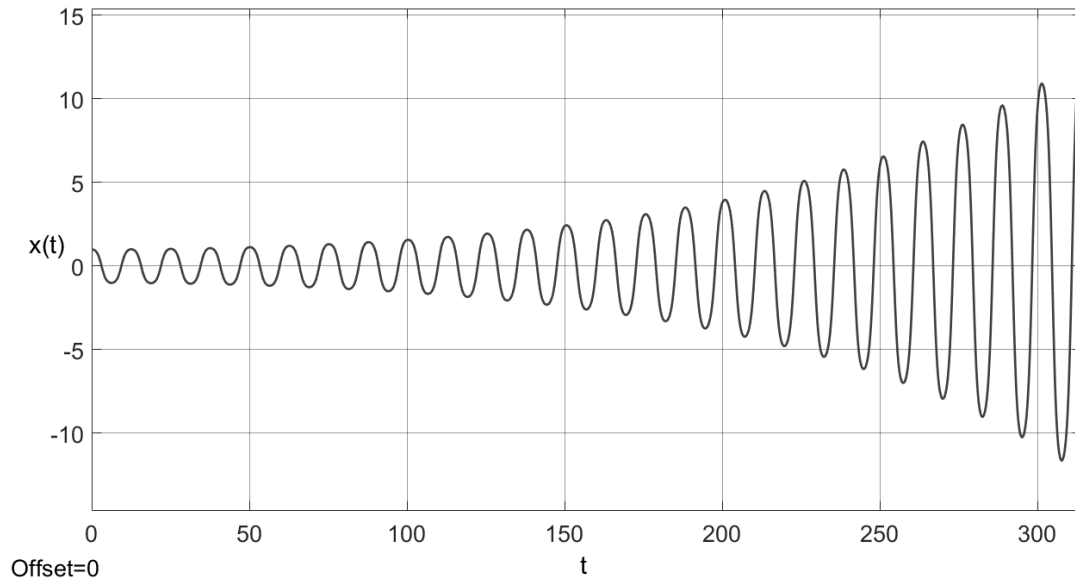


Figure 6.3: Unbounded solution for the elastic shaft system.

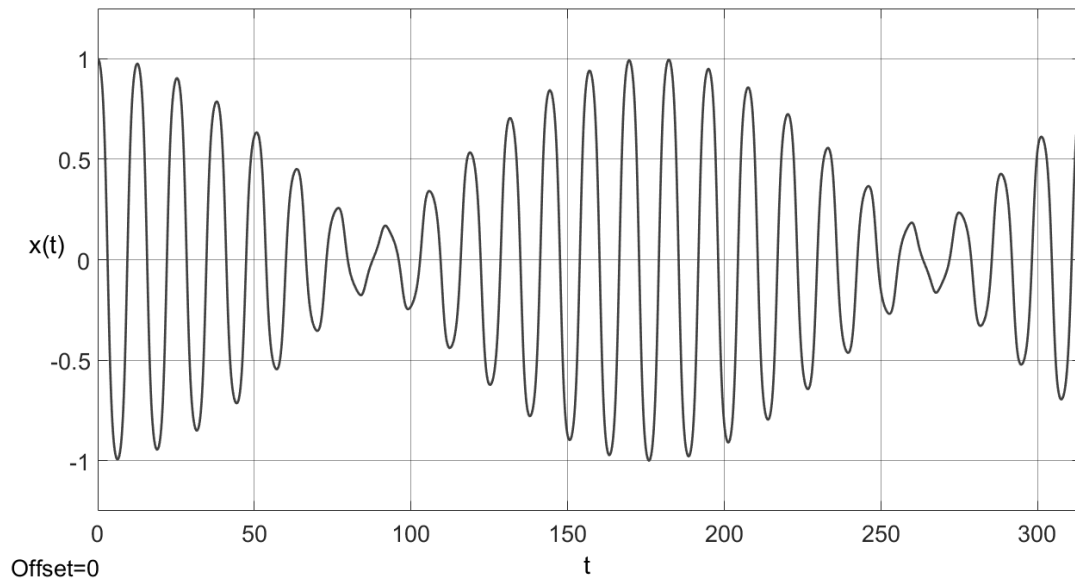


Figure 6.4: Bounded solution for the elastic shaft system.

# Chapter 7

## An application of the Mathieu equation

### 7.1 Quadrupole mass filter

The quadrupole mass filter is the main device inside the quadrupole mass spectrometer. This filter consists of four metal rods arranged as in Fig. 7.1. An electric potential  $\phi_0(t)/2$  is applied to the pair of horizontally opposing rods, and  $-\phi_0(t)/2$  to the vertically opposing rods, where  $\phi(t) = U + V \cos(\omega t)$ . The motion of an ion passing through the rods is modeled by two decoupled Mathieu equations. From the Ince-Strutt diagram of these equations, a pass-band filter is designed. Only ions which have a mass to charge ratio, within a narrow interval of values, called a stable interval of mass to charge ratios, pass all the way through the filter, while the others either collide to the electrodes or exit laterally. The principle of operation of this filter can be applied to other devices such as the ion trap. The theory of both the filter and the trap devices is found in [23].

For mass spectrometry, ions are obtained by an ionization process applied on a sample of the substance to be analyzed, and they are passed between the filter rods by means of an ion accelerator. A scanning process is executed through a wide range of mass to charge ratios. A detector measures the electrical signal generated by the ions that were able to pass all the way through the filter, which finally allows to plot the mass spectrum of the substance.

#### 7.1.1 Ion equations of motion

Consider an electric field

$$E = -\frac{\partial \phi}{\partial u}$$

where  $\phi(t, u) \in \mathbb{R}$  is the potential at any point  $u = [x, y, z]^T$  within the field.

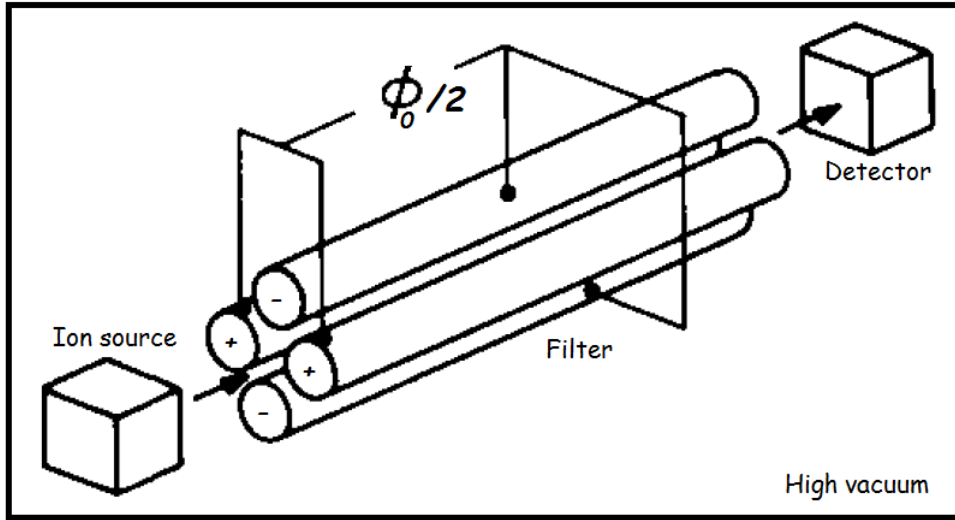


Figure 7.1: Schematic of the quadrupole ion mass spectrometer (image borrowed and modified from [23]).

For a quadrupole field, the potential  $\phi$  is

$$\phi = \frac{\phi_0}{2r_0^2} (\sigma_x x^2 + \sigma_y y^2 + \sigma_z z^2) \quad (7.1)$$

where  $\phi_0$  is the electric potential applied to the electrodes,  $r_0$  is half the distance between each opposite rod, and  $\sigma_x$ ,  $\sigma_y$  and  $\sigma_z$  are weighting constants. Fig. 7.2 shows the ideal shape of the electrodes in order to obtain (7.1).

From Gauss' law, the quadrupole electric field satisfies

$$\text{div}(E) = 0,$$

where  $\text{div}$  is the divergence operator, since the charge density is null inside the quadrupole filter, then

$$\text{div} \left( \frac{\partial \phi}{\partial u} \right) = 0 \quad (7.2)$$

which is Laplace equation.

In order to satisfy (7.2), the weighting constants must satisfy  $\sigma_x + \sigma_y + \sigma_z = 0$ . For the mass filter:  $\sigma_x = -\sigma_y = 1$ ,  $\sigma_z = 0$ , whilst for the quadrupole ion trap:  $\sigma_x = \sigma_y = 1$ ,  $\sigma_z = -2$ .

The field  $E$  in a quadrupole device is uncoupled so that the forces in the three coordinate directions may be determined separately. The force,  $F_x$ , in the  $x$  direction, experienced by an



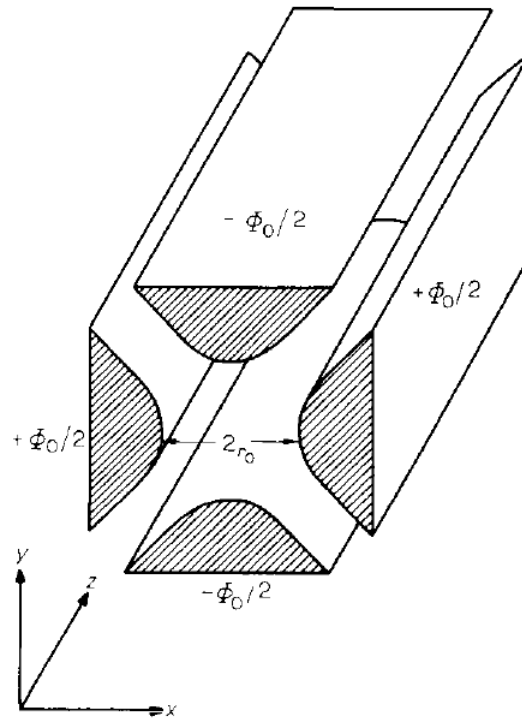


Figure 7.2: Ideal shaped electrodes for the potential (7.1) (image borrowed from [23]).

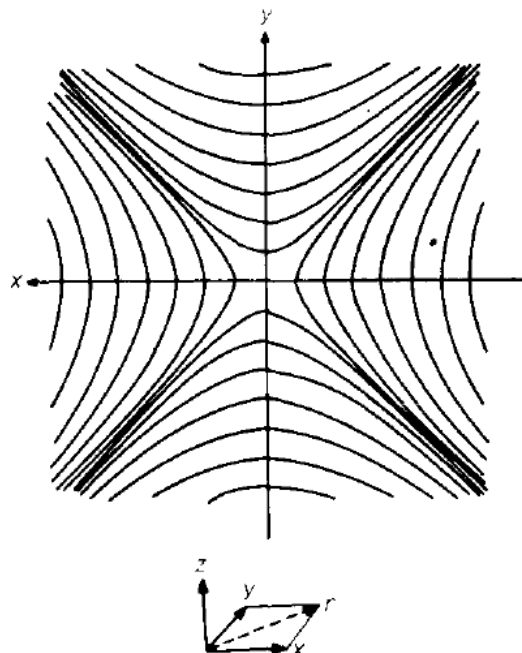


Figure 7.3: Equipotential lines for a quadrupole field with the potential (7.1) (image borrowed from [23]).

ion of mass  $m$  and charge  $q$  at any point within a quadrupole field is then

$$F_x = ma_x = m \frac{d^2x}{dt^2} = qE = -q \frac{\partial \phi}{\partial x} \quad (7.3)$$

where  $a_x$  is the acceleration of the ion in the  $x$ -direction.

From (7.3) and (7.1), the equations of motion of an ion passing through the quadrupole filter are

$$\frac{d^2x}{dt^2} + \frac{q\phi_0}{mr_0^2}x = 0$$

$$\frac{d^2y}{dt^2} - \frac{q\phi_0}{mr_0^2}y = 0$$

$$\frac{d^2z}{dt^2} = 0$$

If  $\phi_0(t) = U$ , a positive *D.C.* voltage, then the motion of an ion (cation) at the  $x$  direction will be stable, and unstable at the  $y$  direction. But, if instead  $\phi_0 = U + V \cos(\omega t)$ , with  $U > 0$ ,  $V > 0$ , then the equations of motion in the  $x$  and  $y$  directions become the Mathieu equations

$$\frac{d^2x}{d\tau^2} + (\alpha + 2\beta \cos(2\tau))x = 0 \quad (7.4)$$

$$\frac{d^2y}{d\tau^2} - (\alpha + 2\beta \cos(2\tau))y = 0 \quad (7.5)$$

where  $\tau = \omega t/2$ ,  $\alpha = 4qU/(mr_0^2\omega^2)$ ,  $\beta = 2qV/(mr_0^2\omega^2)$ .

Figure 7.4 shows the superimposed Ince-Strutt diagrams of the equations of motion (7.5) (in red, at the background) and (7.4) (in blue). Both Ince-Strutt diagrams are symmetric with respect to the  $\beta$  axis. White areas correspond to stable parameter regions for both the  $x$  and  $y$  directions. The larger white region in Figure 7.4 will be called, in the following, as the operating region of the filter.

## 7.1.2 Filtering principle

Notice that  $\beta/\alpha = V/(2U)$ . For fixed values of  $\omega$ ,  $U$  and  $V$ , all ions with the same mass-to-charge ratio correspond to the same point in the  $\alpha - \beta$  plane, and the variation of mass-to-charge ratio, produced by the different ions passing between the electrodes of the filter, move the parameters  $\alpha$  and  $\beta$  of the equations of motion along the line of slope  $V/(2U)$ , called the operating line of the filter, shown as a dashed line in Figure 7.5. Only those ions whose

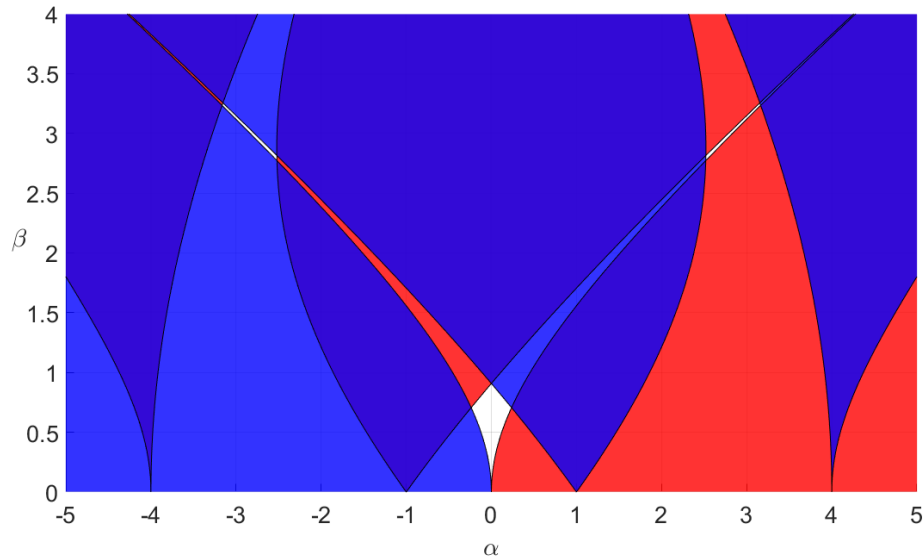


Figure 7.4: Ince-Strutt diagram of the quadrupole mass filter

mass-to-charge ratio sets  $\alpha$  and  $\beta$  inside the operating region are allowed to pass all the way through the filter. Thus the section of the operating line passing through the operating region of the filter determines the interval of stable mass-to-charge ratio values.

The resolution of the filter is determined by the value of  $V/(2U)$ . A smaller value of  $V/(2U)$ , so that the operating line still passes through the operating region, makes a smaller interval of values of mass-to-charge ratio to correspond to stable ion trajectories.

For the scanning process (once the desired resolution is chosen), the modification of the magnitude of  $V$  and  $U$ , so that its ratio stays constant, changes the limits of the interval of mass-to-charge ratio values inside the operating region. For example, if  $V$  and  $U$  are both simultaneously doubled, the new stable mass-to-charge ratio interval contains the values of the old interval but doubled.

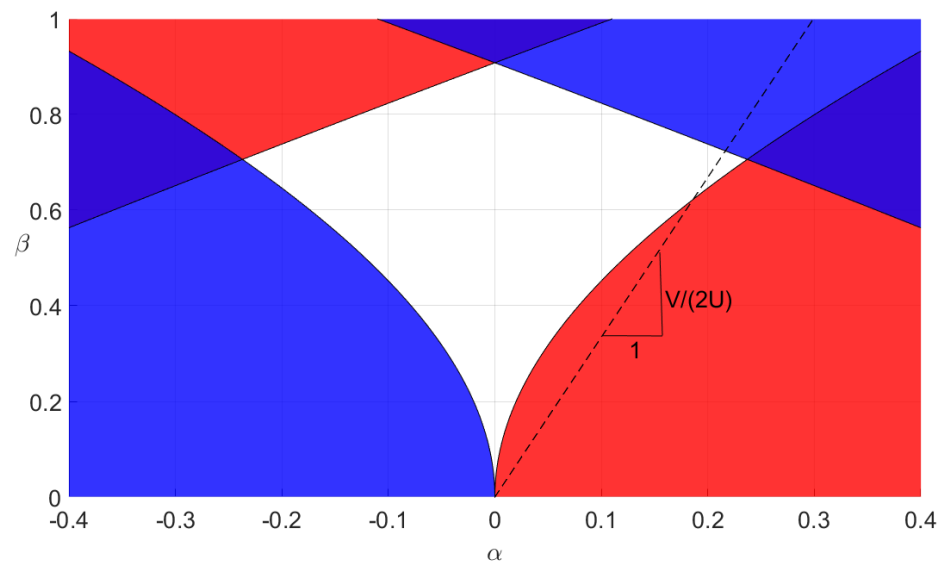


Figure 7.5: Filter calibration line

# Chapter 8

## Conclusions and future work

### 8.1 Conclusions

For a fixed value of  $\beta$ , it was shown that those values of  $\alpha$ , for which a constant  $\mu \in \mathbb{C}$ ,  $|\mu| = 1$ , is a Floquet multiplier of the Hill equation (1.3), can be computed by solving a twisted Sturm-Liouville problem, whose solutions form a monotonic sequence of real numbers. And from this fact:

- Particular cases of the twisted BCs, for which  $\mu = 1$  and  $\mu = -1$ , called periodic and anti-periodic BCs, respectively, allowed us to find the Ince-Strutt diagram of the Hill equation in the standard form (1.3). Some numerical results, obtained using a finite-difference solution scheme, were presented, and showed six to eight digits of precision when compared with the ones obtained by the spectral differentiation method and Jazar's algorithm.
- The twisted Sturm-Liouville problem, for which  $\text{Im}(\mu) \neq 0$ , was shown useful in order to compute all the splitting lines lying inside the stable regions of parameters, including those associated with aperiodic solutions. Thus, through the solution of a twisted Sturm-Liouville problem, one is able to obtain more information about the behavior of the solutions inside the stable regions of parameters of an Ince-Strutt diagram than that obtained by Jazar's method or the spectral differentiation method.
- Since the Hill equation can be regarded as a particular case of the Sturm-Liouville equation, the Floquet theory and the solution of the periodic and the anti-periodic Sturm-Liouville problems can be used in order to find the bifurcation diagram of a bi-parametric linear periodic second order ordinary differential equation that is not on

a Hill type form, such as the one that models the motion of a mechanical system with periodically time-varying moment of inertia.

- Since the Floquet theory, and hence Floquet multipliers, are not defined for the quasi-periodic Hill equation, the transition curves of this equation, if exist, can not be related with the periodic or the anti-periodic Sturm-Liouville problem.

## 8.2 Future work

- The presented finite-difference scheme could be upgraded in order to compute the principal resonance tongues of the multiple degree of freedom Hill equation [22]. And it could be possible that there exist some particular equations for which the twisted BVP is applicable for the computation of its combination resonance tongues.
- The effect of small perturbations, in the Hamiltonian of the Hill equation, on the long time behavior of its bounded solutions should be studied in order to judge its applicability and to enrich its understanding.

# Bibliography

- [1] W. Magnus and S. Winkler, *Hill's Equation*. Interscience Publishers, a division of John Wiley and Sons, 1966.
- [2] G. W. Hill, *On the Part of the Motion of the Lunar Perigee Which is a Function of the Mean Motions of the Sun and Moon*. Acta Mathematica, vol. 8, pp. 1-36, 1886.
- [3] G. Floquet, *Sur les Equations Differentielles Lineaires a Coefficients Periodiques*. C. R. Acad. Sci Paris 91, pp. 880-882, 1880.
- [4] A. Champneys, *Dynamics of Parametric Excitation*. Math. of Comp. and Dyn. Sys., pp. 183-204, 2011.
- [5] D. W. Jordan and P. Smith, *Nonlinear ordinary differential equations*, 4th ed. New York, United States: Oxford University Press, 2007.
- [6] G. N. Jazar, *Stability Chart of Parametric Vibrating Systems Using Energy-Rate Method*. International Journal of Non-Linear Mechanics, vol. 39, pp. 1319-1331, 2004.
- [7] L. N. Trefethen, *Spectral Methods in Matlab*. SIAM, 2000.
- [8] H. B. Keller, *Numerical Methods for Two-Point Boundary-Value Problems*. Blaisdell Publishing Company, a division of Ginn and Company, 1966.
- [9] G. Birkhoff, C. De Boor, B. Swartz, B. Wendroff, *Rayleigh-Ritz Approximation by Piecewise Cubic Polynomials*. J. SIAM Numerical Analysis, volume 3, number 2, 1966.
- [10] J. Canosa, R. Gomez de Oliveira, *A New Method for the Solution of the Schrödinger Equation*. Journal of Computational Physics, volume 5, 1970, pages 188-207.
- [11] S. Pruess, *Estimating Eigenvalues of Sturm-Liouville Problems by Approximating the Differential Equation*. SIAM Journal of Numerical Analysis, volume 10, number 1, Mar. 1973, pages 55-68.
- [12] R. W. Brockett, *Finite Dimensional Linear Systems*. John Wiley and Sons, 1970.
- [13] W. J. Rugh, *Linear System Theory*, 2nd ed. Prentice Hall, 1996.
- [14] L. Ya. Adrianova, *Introduction to Linear Systems of Differential Equations*. American Mathematical Society, 1995.
- [15] B. M. Brown, M. S. P. Eastham, K. M. Schmidt, *Periodic Differential Operators*. Birkhäuser, 2012.

- 
- [16] K. R. Meyer, G. R. Hall and D. Offin, *Introduction to Hamiltonian Dynamical Systems and the N-Body Problem*, 2nd ed. Springer, 2009.
- [17] A. C. Dixon, *The Elementary Properties of the Elliptic Functions with Examples*. Macmillan and Co. 1894.
- [18] S. B. Yuste, *Métodos Matemáticos Avanzados para Científicos e Ingenieros*. Universidad de Extremadura, 2006.
- [19] E. A. Coddington, N. Levinson, *Theory of Ordinary Differential Equations*. Tata McGraw-Hill, 1987.
- [20] B. Fornberg, *Generation of Finite Difference Formulas for Arbitrarily Space Grids*. Mathematics of computation, volume 51, number 184, october 1988, pages 699-706.
- [21] A. Rodriguez, and J. Collado, *On Stability Of Periodic Solutions in Non-homogeneous Hill's Equation*. Mexico City, 12th International Conference on Electrical Engineering, Computing Science and Automatic Control (CCE), 2015.
- [22] A. P. Seyranian, *Parametric Resonance in Mechanics: Classical Problems and New Results*. Journal of system design and dynamics, volume 2, number 3, 2008.
- [23] P. H. Dawson, *Quadrupole Mass Spectrometry and its Applications*. Elsevier Scientific Publishing Company, Amsterdam-Oxford-New York, 1976.